FT-IR Spectroscopy Technology, Market Evolution and Future Strategies of Bruker Optics Inc.

by

Thomas Higdon

B.S. Physics, McGill University, 2002

Submitted to the System Design and Management Program
in Partial Fulfillment of the Requirements for the Degree of

Master of Science in Engineering and Management

at the

Massachusetts Institute of Technology

April 2010
[June 2010]

Signature of Author _____

Thomas Higdon
System Design and Management Program
April 27, 2010

Certified by _____

Christopher L. Magee
Professor of the Practice
Engineering Systems Division
Thesis Supervisor

Accepted by _____

Patrick Hale
Director
System Design & Management Program

FT-IR Spectroscopy Technology, Market Evolution and Future Strategies of Bruker Optics Inc.

by

Thomas Higdon

Submitted to the System Design and Management Program
on April 23, 2010 in Partial Fulfillment of the
Requirements for the Degree of Master of Science in
Engineering and Management

Abstract

This thesis explores the technology and market evolution of FT-IR spectroscopy over its nearly forty year history to aid in determining future product design and marketing strategies for an industry-leading firm, Bruker Optics. As a benchmark, a universal performance metric was developed that combined key specifications applicable to all FT-IR spectrometers. By researching a selected set of Bruker Optics' spectrometer systems, this performance benchmark was calculated along with each instrument's weight, volume, power consumption, and cost. The universal performance curve displayed an exponential increase from 1974 to 1988, but the rate of improvement has since decreased dramatically to incremental increase in the last twenty years.

Using Design Structure Matrix analysis, the architectural trends of the same instruments were traced to discern the impact an instrument's overall design had on its performance. This analysis resulted in no definitive correlations between a spectrometer's performance and its architecture. Rather the overall instrument performance increases were attributable to individual component performance increases. However, with respect to volume, power consumption, and cost, there were clear correlations to instrument architecture. While spectrometer weight was fairly consistent over the years, decreasing instrument volume coincided with decreasing part count. Likewise, power consumption decreases over the past twenty years corresponded with decreasing energy and informational links within each instrument's architecture. The most striking correlation was the nearly perfect linear relationship between decreasing cost and decreasing instrument matter/spatial link count.

Over the past fifteen years, incremental performance increase coupled with exponentially decreasing cost has resulted in FT-IR spectrometers becoming more and more commoditized. Consumers expect high performance at low cost which jeopardizes future profitability and growth for companies in the increasingly competitive FT-IR market. Bruker Optics must look to capture greater market share in segments outside of the research segment it currently dominates. By shifting from their historically product-oriented culture to a more market-oriented one, and by specifically targeting the near Infrared scanner segment, Bruker Optics will be primed for future success.

Thesis Supervisor: Christopher L. Magee
Title: Professor of the Practice of Mechanical Engineering and Engineering Systems

Acknowledgements

I would like to first thank Dr. Chris Magee who has been an incredibly helpful and understanding advisor. This thesis has been through many changes and iterations mainly due to it being a secondary thesis topic. After months of work, the original topic fell through last minute due to lack of data from the source company. Professor Magee was very understanding of my situation and helped shape this thesis to its current state. I am very thankful for his help and guidance.

I want to thank the SDM professors, staff, and fellow classmates who have shared their time, knowledge, and experiences. Without their input, I would not have learned nearly as much I have in the program.

I also would like to thank my former coworkers at Bruker Optics for their time and allowing me access to their instruments and documentation. In an industry that keeps tight control over its performance specifications and latest designs, their willingness to participate is greatly appreciated. Without them, this thesis would not have been possible. I hope they find the results, analysis, and strategies in this thesis useful in their future endeavors.

Last, but certainly not least, I would like to thank my parents and friends who have been very supportive of me throughout my entire life. Without their support, this past year and a half in the SDM program would have been much more difficult to complete.

Table of Contents

List of Figures

List of Tables

List of Equations

1 Introduction

1.1 Motivation / Purpose

As a former employee to an industry leader in the Fourier Transform Infrared (FT-IR) spectrometer market, I wanted to study FT-IR spectrometer performance trends over time and characterize them relative to architectural trends. By utilizing some of the system analysis tools and technology strategy methods acquired from the System Design and Management (SDM) program, my general approach was to find answers to the following three questions:

- What are the historical technological and architecture trends of Bruker Optics' FT-IR spectrometers?
- Are there correlations between these technological and architecture trends?
- Based on the technological and architectural analysis, what future product design and marketing strategies should Bruker Optics pursue?

It seems to be a common assumption that FT-IR spectrometer performance has increased over time since they were first commercially available in the mid 1970's, especially with regard to the computing and signal processing components. However, there is little empirical evidence of performance increases outside of the aforementioned components. This thesis will generate performance data through the analysis of four research-grade spectrometer systems produced by a market leading spectrometer firm, Bruker Optics Inc. These four specific systems were chosen because they were a representative sampling of the firm's premier product line over its nearly forty year history. Before delving into the thesis approach and results of the analysis of these systems, some basics about Infrared spectroscopy is covered in the following five sections.

1.2 Infrared Spectroscopy Theory

Infrared or IR spectroscopy is a specialized method of molecular spectroscopy. Molecular spectroscopy theory relies on the principle that molecular rotations and vibrations of chemical compounds absorb specific frequencies of electromagnetic waves. One particular portion of the electromagnetic spectrum, the Infrared, is especially suitable for the detection of molecular vibrations. The IR spectrum refers to electromagnetic waves whose wavelengths range from 0.78

μm to 1000 μm (1). For more manageable numbers, the wavenumber unit (cm^{-1}) is generally used instead of microns so the total IR spectrum is from 14,286 cm^{-1} to 28.5 cm^{-1}. The IR spectrum is further divided in three sections: near infrared (NIR), mid infrared (MIR), and far infrared (FIR). Table 1 below displays the ranges of the IR spectrum.

Infrared Section	Wavelength Range (μm)	Wavenumber Range (cm^{-1})
Near Infrared (NIR)	0.78 – 2.5	12,821 – 4,000
Mid Infrared (MIR)	2.5 – 50	4,000 - 200
Far Infrared (FIR)	50 - 1000	200 - 10

Table 1: Infrared Spectral Ranges (1)

As stated in the previous paragraph, the IR spectrum is ideal for detecting molecular vibrations in liquids or solids. These molecular vibrations can be split into two categories: stretching and bending. Stretching vibrations are categorized as symmetric or asymmetric and bending vibrations are characterized as rocking, scissoring, wagging, or twisting (1). Figure 1 below displays different modes of vibration for a simple molecule with arrows demonstrating the particular motions.

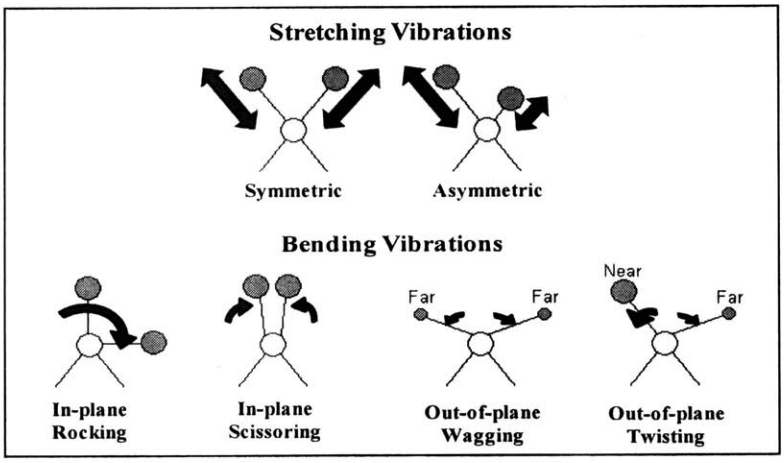

Figure 1: Types of Molecular Vibration (1)

Each of a molecule's modes of vibration occurs at a specific frequency and will consequently absorb electromagnetic radiation of this frequency. These unique frequency absorptions result in a characteristic spectral profile for a given molecule or molecular compound. Figure 2 below

displays a MIR spectral profile of formaldehyde where each absorption band is labeled with its specific vibration mode and corresponding frequency in cm^{-1}.

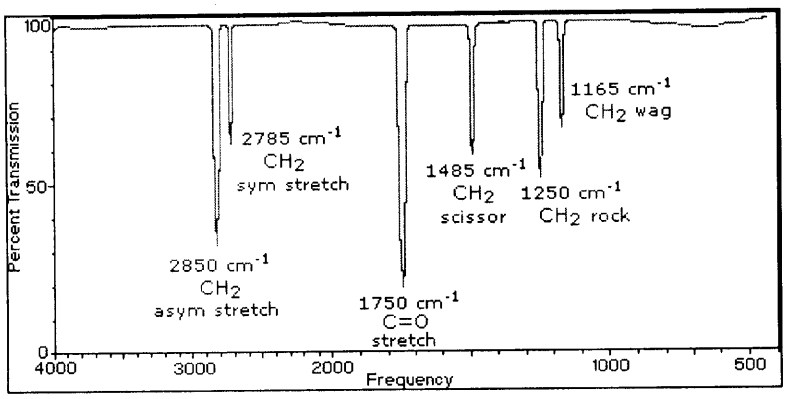

Figure 2: MIR Spectrum of Formaldehyde (2)

1.3 Infrared Spectroscopy Implementation

It is obvious from looking at the example MIR spectrum of formaldehyde that IR spectroscopy's capability to accurately identify specific molecules and compounds is ideal for a wide variety of applications. Historically, IR spectroscopy has been made possible using two types of spectrometers: dispersive or Fourier Transform. Both spectrometers use similar components, but the method in which spectral data is captured is inherently different. Dispersive IR spectrometers utilize a monochromator, which is a device that filters incoming IR frequencies of radiation to output a specific frequency. Figure 3 below is an example of a simple dispersive IR spectrometer layout.

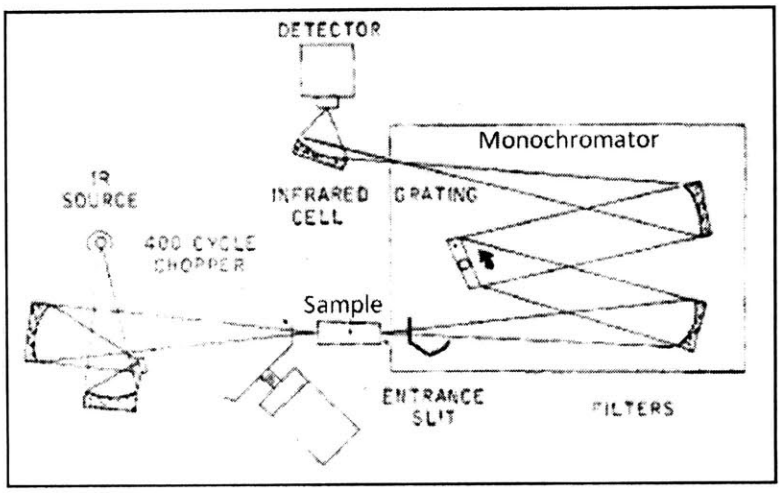

Figure 3: Dispersive IR Spectrometer Layout (3)

Similarly to an FT-IR spectrometer, the energy path in a dispersive IR spectrometer initiates from the IR source. IR radiation generated by the source passes a chopper wheel before illuminating the sample. The chopper either allows or blocks the IR radiation and acts as a trigger for the detector to initiate data collection. After passing through the sample, the IR radiation then enters a monochromator. The monochromator is composed of an entrance slit aperture, a grating to reduce incoming frequencies to a specific frequency, and an exit slit aperture. It essentially acts as a variable optical filter. Once exiting the monochromator, a detector then records the sample's absorbance of the particular frequency of IR radiation. The monochromator is then adjusted to output a different frequency and the detector records the absorption level of the new frequency. This process is repeated until the desired frequency range is covered.

Compared to traditional dispersive IR spectrometers, FT-IR spectrometers have three main advantages. They enable quicker data collection, have higher IR throughput, and offer greater precision due to a reliable internal calibration source. These three advantages are a result of the implementation of a laser-referenced interferometer instead of a monochromator. Unlike a monochromator, an interferometer allows all desired frequencies to be recorded by the detector at each data sampling point which allows faster data collection. The interferometer also allows greater IR radiation intensity through to the detector because it does not attenuate the IR signal in any way. A monochromator greatly attenuates IR radiation intensity due to the slits at its input

and output. In addition, the laser, which is part of the interferometer control system, is a reliable calibration source because of its consistent wavelength.

Recent advancements in micro electro-mechanical systems (MEMS) manufacturing has given rise to a new type of dispersive spectrometer. MEMS spectrometers essentially function in the same manner as traditional dispersive IR spectrometers except that the frequency filter grating is an electronically controlled pixel array. A layout of a MEMS pixel array is shown in Figure 4 below.

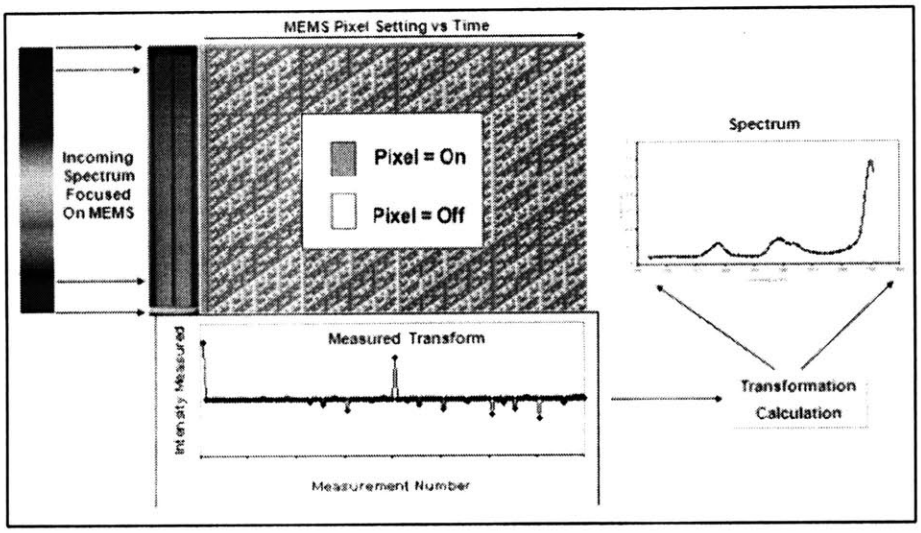

Figure 4: MEMS Spectrometer Layout (4)

IR radiation from the sample hits the MEMS pixel matrix whose rows represent time samples and whose columns represent spectral ranges. Different spectral ranges are achieved by combinations of pixel on/off patterns which enables quick measurements across multiple spectral bands. The IR radiation continues to the detector which measures the IR intensities. This data is then processed using a digital transform to produce a spectrum. MEMS spectrometers are extremely small in size, consume very little power, and require no moving parts. Although they are still in their early stages of development, MEMS spectrometers look to challenge FT-IR spectrometers as the dominant technology of the future.

1.4 FT-IR Spectrometer Basics

All FT-IR spectrometers, in their simplest configurations, are composed of the following components: source(s), mirrors, interferometer, detector(s), and signal processor. Please refer to Figure 5 below which displays the optical layout of a simple spectrometer.

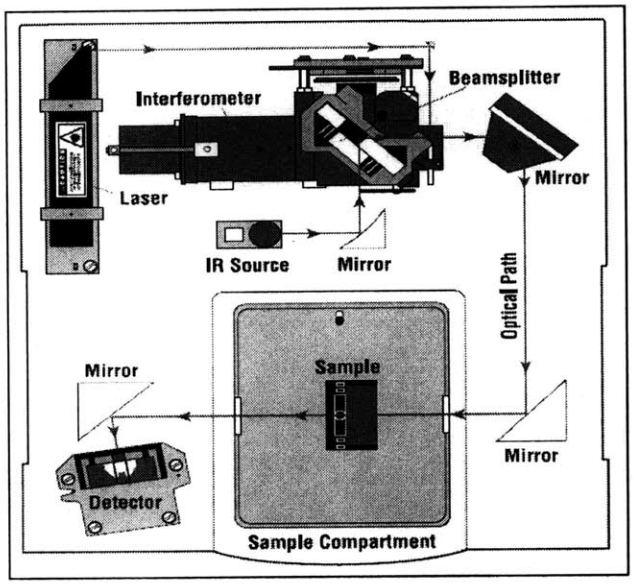

Figure 5: Basic FT-IR Spectrometer Layout (5)

A source, most commonly a globar, provides the Infrared or heat radiation which is directed by mirrors into the interferometer. Figure 6 is an example of a Michelson interferometer complete with IR radiation and laser beam paths. The Michelson interferometer, which was named after its inventor Albert Michelson (6), can be further decomposed into a beam splitter, a moving mirror, and a stationary mirror. The interferometer splits incoming radiation into two paths and recombines them to produce an interference pattern, which is commonly referred to as an interferogram shown in Figure 6 below. One path has a constant length, determined by a fixed mirror and the other path has variable length which is determined by a moving mirror. The optical path difference (OPD) is the difference between the fixed path length and the variable path length (7). Since the fixed path is constant, it follows that a higher OPD can only be achieved through a longer variable path or larger moving mirror range.

The remaining component shown in both Figure 5 and Figure 6, the laser, is used for controlling the interferometer's moving mirror and data sampling points. A Helium Neon

(HeNe) laser is commonly used because of its availability and cost. The laser signal is also split and recombined by the interferometer just like the IR radiation, but because the laser has a specific wavelength and subsequent frequency, the recombination results in alternating constructive and destructive interference shown in Figure 6. These dark areas or destructive interference points are used both as references to determine the moving mirror's travel distance, and as trigger points for the detector to sample data.

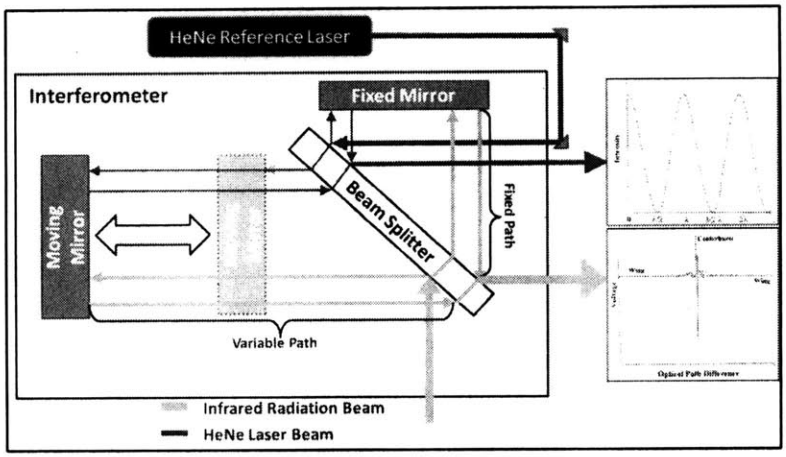

Figure 6: Michelson Interferometer[1]

Once the Infrared radiation has passed through the interferometer, it illuminates the sample, which either absorbs or transmits frequencies of the spectrum which continue to the detector where the IR radiation is converted to an analog voltage signal. Detectors are split into two categories depending on the detection methodology. Thermal, the first type, uses a conductor or semiconductor whose resistance changes depending on temperature changes. One example of a commonly used thermal detector in modern IR spectroscopy is dueterated triglycine sulfate or DTGS. Thermal detectors have been widely used over the past century, but they do have a significant drawback which is response time. Typical response times of milliseconds limits the sampling rates of the detector (8). For faster sampling requirements, a second category of detector, the quantum type, is used.

Quantum detectors rely on the principle that radiation causes the excitation of the electrons in a material to higher, quantized energy states. The energy of the incident radiation photons is directly proportional to its wavelength. By measuring the voltage of the quantum detector, one

[1] (8), (9)

can determine the wavelength of the incident radiation. These detectors are far more sensitive and have shorter response times than thermal ones, but generally require cooling to eliminate background noise in the detection material (8). The most commonly used quantum detector is mercury cadmium telluride (MCT) which requires cooling by liquid nitrogen.

After the detector converts the IR radiation to a voltage, this voltage signal is then converted into "understandable" digital data by the signal processor through amplification, analogue to digital conversion, and Fast Fourier Transform (FFT) algorithms. The FFT integrates time-domain interferogram data to generate frequency-domain spectrum data shown in Figure 7 below.

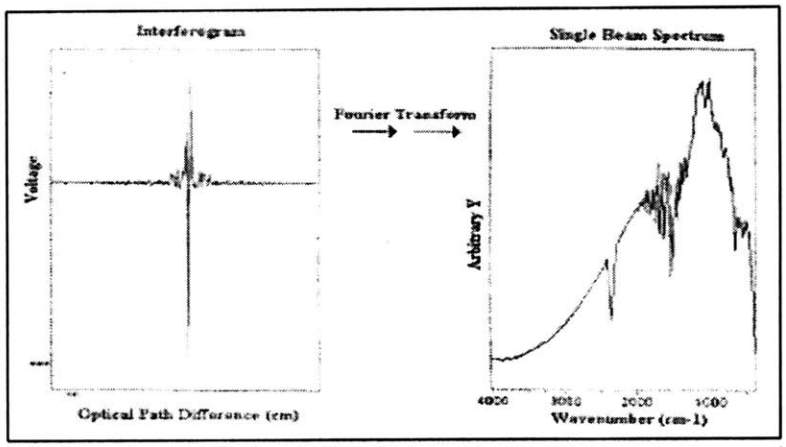

Figure 7: FFT Conversion (9)

Since the data from the detector is sampled at discrete points in time rather than continuously sampled, integration of the interferogram has to also be done by a series of Discrete Fourier Transforms (DTF)s. The general equation for calculating a DFT is shown below. B(r) is Fourier Transformed spectrum in terms of wavenumbers, r.

$$B(r) = \sum_{k=0}^{N-1} S_0(k) W^{rk}$$

S_0 *is the value of the inteferogram at point* k,

$$W = e^{-i2\pi/N},$$

r is the wavenumber of the k^{th} point

Equation 1: Discrete Fourier Transform (8)

Each discrete value of *B(r)* requires *N* multiplications and *N*-1 additions. Since there are also *N* terms of *B(r)*, the DFT equation requires N^2 complex multiplications (8). These required complex multiplications can quickly become implausible for large values of *N* even for modern day computers. For example, a spectrum of 10^6 sampling points would require 10^{12} DFT calculations. However, Cooley and Tukey's FFT algorithm significantly reduces the calculation operations by using base 2 values for *N*. For values of $N = 2^{\alpha}$, the ratio of DFT to FFT complex multiplications is shown in Equation 2 below.

$$\frac{N^2}{\frac{N\alpha}{2}} = \frac{2N}{\alpha} \; ; \; \forall \, \alpha = 1, 2, 3, \ldots$$

Equation 2: Ratio of DFT to FFT Complex Multiplications (8)

It follows from Equation 2 that for $\alpha = 1$, the FFT algorithm reduces complex calculations in half relative to the number of DFT calculations. The FFT's large reduction in complex calculations enabled early computers to generate spectra in reasonable periods of time.

From the general architecture, an FT-IR spectrometer can theoretically support the entire IR spectrum. However, due to material characteristics, a single configuration of a source, beam splitter, and detector will not allow data collection over the entire IR range. Certain materials will not transmit or reflect IR signal, but rather block or absorb them. Other materials are transparent to specific ranges of the IR spectrum which make them ideal for FT-IR use. As a result, most commercially available FT-IR spectrometers are modularly designed so the sources, beam splitter, and detectors are interchangeable allowing the spectrometer to be tuned or customized to support multiple portions of the IR spectrum. Table 2 below contains common IR components and their respective supporting IR spectral ranges.

Component Type	Component Name	Material	Spectral Range
Source	Mercury Arc Lamp	Mercury Gas	FIR
Source	Globar	Silicon Carbide	FIR/MIR
Source	Tungsten Lamp	Tungsten	MIR/NIR
Source	Xenon Arc Lamp	Xenon Gas	VIS/UV
Mirror	Mirror	Gold Coated	FIR/MIR/NIR
Mirror	Mirror	Aluminum Coated	MIR/NIR/VIS/UV

Beam Splitter	Mylar™	Mylar™	FIR
Beam Splitter	KBr	Germanium-Potassium Bromide	MIR
Beam Splitter	CaF_2	Calcium Fluoride	MIR/NIR/VIS
Beam Splitter	Quartz	Quartz	VIS/UV
Detector	Bolometer	Silicon Photodiode	FIR/MIR
Detector	DTGS	Deuterated Triglycine Sulfate	FIR/MIR
Detector	MCT	Mercury Cadmium Telluride	MIR
Detector	InSb	Indium Antimonide	MIR/NIR
Detector	InGaAs	Indium Gallium Arsenide	NIR
Detector	Si-Diode	Silicon Diode	VIS/UV
Detector	GaP-Diode	Gallium Phosphide	VIS/UV

Table 2: Common FT-IR Spectrometer Components (10)

1.5 Brief History of FT-IR Spectroscopy

Because an FT-IR spectrometer is an integration of several major components, in order to properly trace the technological history of FT-IR spectrometers, one needs to trace the technological advancements of each major component. Figure 8 below includes major technological milestones of these major components: mirrors/optics, interferometers, detectors, and computing hardware and software.

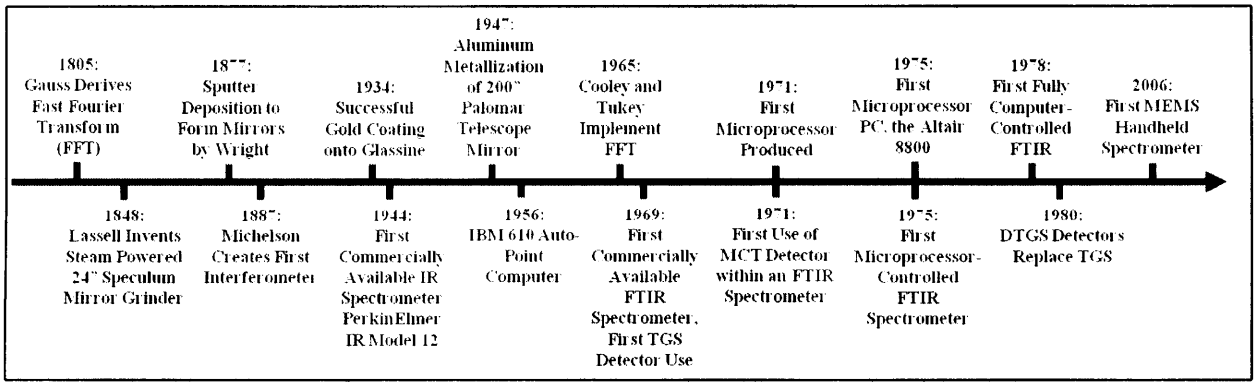

Figure 8: Major Technological Advancements in IR Spectroscopy[2]

Regarding the mirrors and optics, the two greatest technological advances were the development of precision mirror grinding techniques in the late 1840's and vacuum deposition in 1877. These two developments enabled the production of high precision mirrors and beam

[2] (11), (6), (24), (25), (8), (30), (26), (29), (31) , (32), (20)

splitters. Mirrors are often manufactured by grinding a substrate to a specific shape which is then coated with a thin film of optical material. Two common optical coatings used in FT-IR spectrometer mirrors are gold and aluminum which were successfully implemented in 1934 and 1947 respectively (11). A common beam splitter configuration is a thin film of Germanium deposited between two panes of Potassium Bromide.

The interferometer was developed by Albert Michelson in 1887 when he and Edward Morley disproved the existence of "luminiferous ether" (6). Since then, there have been numerous types of interferometers developed, but they all adhere to the same principle used in Michelson's original design. Advancements in the interferometer since its creation have primarily been with the bearing mechanism and scanning control. Mechanical bearings were used initially, but were replaced with virtually frictionless air bearings. Unlike mechanical bearings that require a lubrication substance like oil or graphite, air bearings do not require lubrication, but instead require a pressurized gas source (9). In the first interferometers, the moving mirror was controlled by hand using a micrometer which was difficult to control and highly inaccurate. The development of controlling electronics and a reliable HeNe laser in the 1970s enabled fully processor-controlled scanning.

As mentioned in the previous section, the most common detectors used in FT-IR spectrometers are deuterated triglycine sulfate (DTGS) which is a thermal detector, and mercury cadmium telluride (MCT) which is a quantum detector. However, MCT and DTGS detectors were not widely used until the 1970's and 1980's respectively. Prior to the 1970's, triglycine sulfate (TGS) detectors, the precursors to the DTGS, were used (8).

Computing hardware and software was really the final technological advancement that enabled FT-IR spectroscopy. Prior to the emergence of electronic computers in the 1950's, FT-IR spectroscopy only existed in theory because the FT calculations required to generate spectra were nearly impossible to execute by hand. These early computers, coupled with software implementations of FFT algorithms allowed the calculation intensive generation of spectra to become a reality.

1.6 FT-IR Spectrometer Market

Because FT-IR spectrometers provide a quick, accurate, and cost-effective capability to identify specific molecules and compounds, they are used in almost every industry. Since its nascence in the mid 1900's, the global Fourier Transform Infrared (FT-IR) spectrometer market has grown to $900M in 2008 and is projected to grow to nearly $1 billion in 2010 (12). Despite its relatively small size, there are numerous firms such as Thermo-Nicolet, PerkinElmir, FOSS, Bruker Optics, and JASCO who are in competition for market share. Figure 9 and Figure 10 below display market share by vendor of the Near Infrared (NIR) and Mid/Far Infrared (MIR/FIR) markets. The combined MIR/FIR markets were denoted simply as IR.

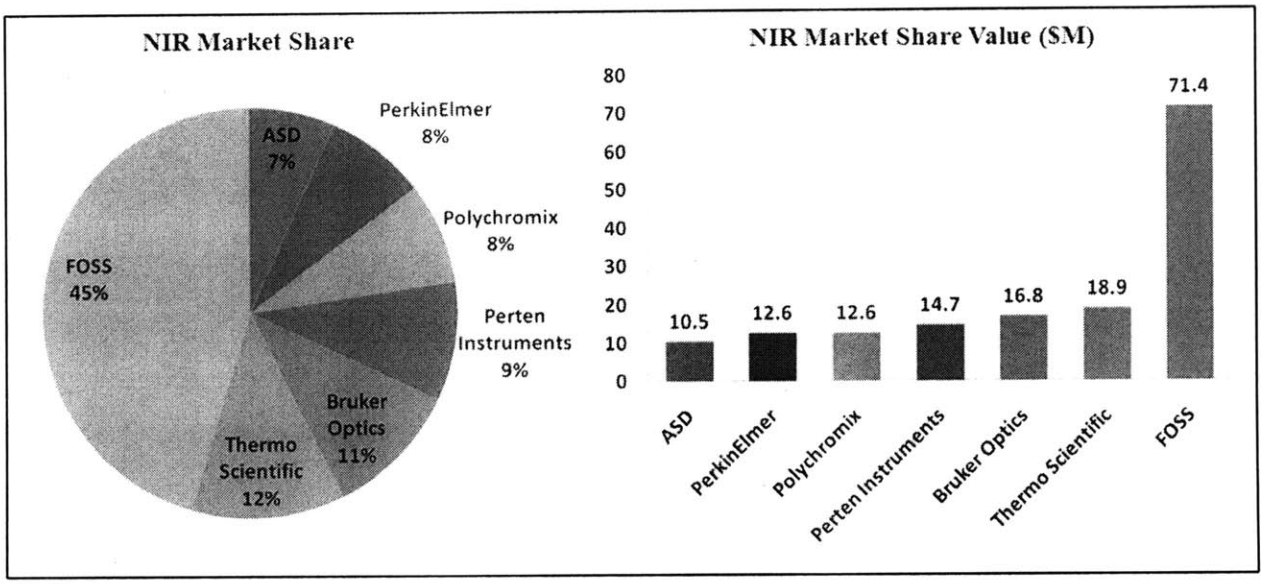

Figure 9: NIR Market Share by Vendor in 2007 (13)

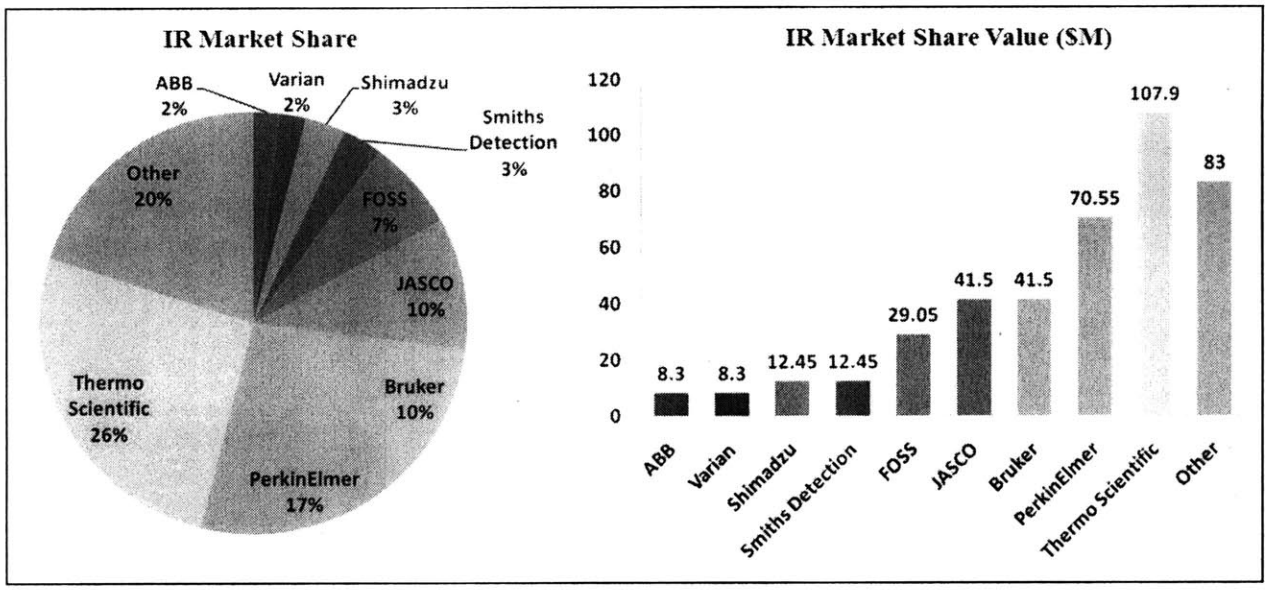

Figure 10: IR Market Share by Vendor in 2007 (13)

In the NIR market, FOSS is the clear leader with 45% followed by Thermo Scientific with 12% and Bruker Optics with 11%. Of the IR market, Thermo Scientific is the leader with 26% followed by PerkinElmer with 17% and Bruker Optics with 10%. Because of the similarity of the products, most spectroscopy companies are present in both the NIR and IR markets. Bruker Optics' combined NIR and IR market revenue was a little over $58M in 2007.

What started out as a tiny research market has evolved and now spans across private, commercial, and government sectors which is evident in the varied application and functional market segments. Figure 11 and Figure 12 below are snapshots of the NIR and IR markets using application, functional, and regional segmentation.

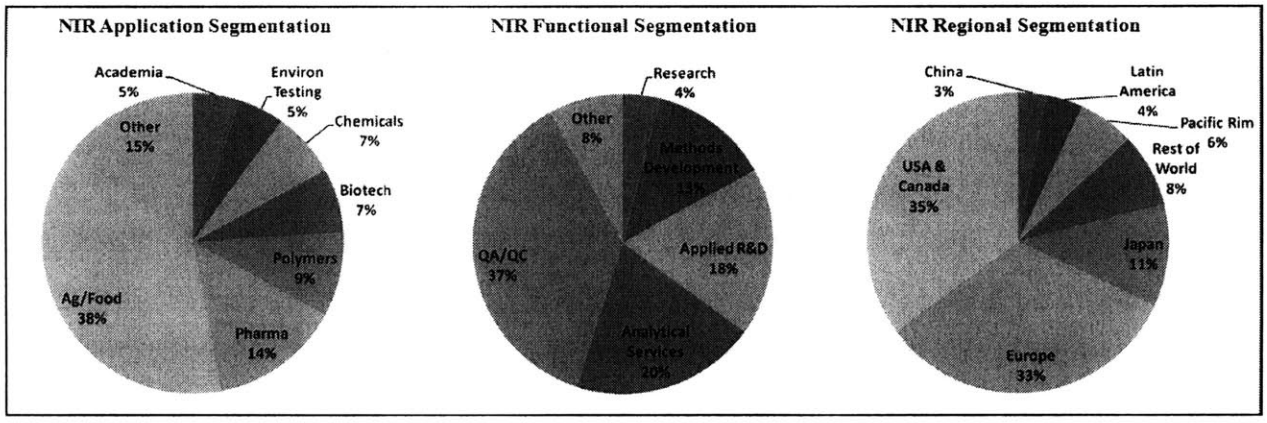

Figure 11: Overview of Global NIR Market in 2007 (13)

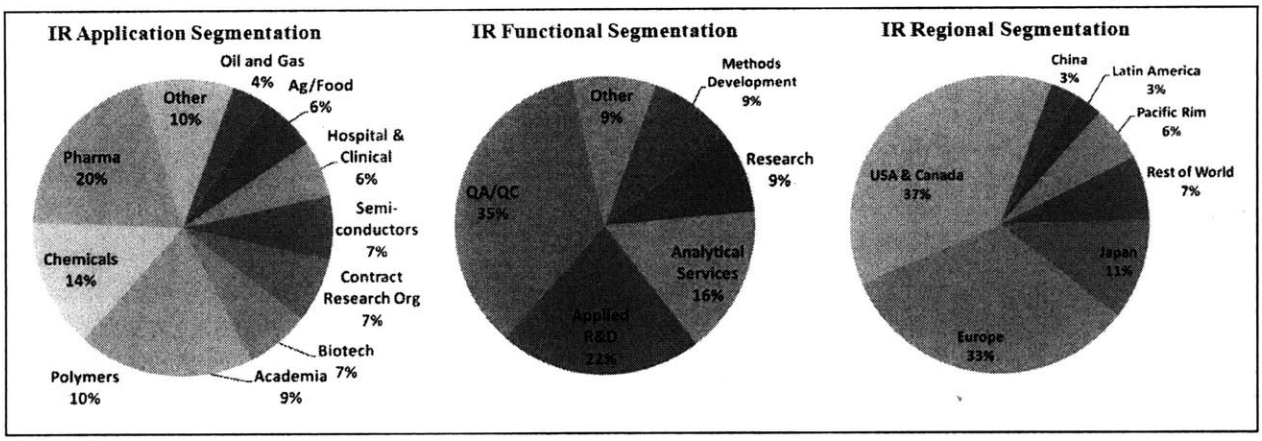

Figure 12: Overview of Global IR Market in 2007 (13)

The total NIR market in 2007 was worth $210M in total new systems. Unlike the NIR market which is dominated by dispersive spectrometers, the IR market is almost exclusively FT-IR systems which totaled $415M in 2007 (13). Both markets share similar regional segmentation distributions. Europe, North America, and Japan represent approximately 80% of the global market. This would suggest that the greatest future market growth will most likely occur in Asian countries other than Japan or Latin America because Europe and North American markets are well established and only growing incrementally. Bruker Optics has traditionally dominated the research segment whose combined NIR and IR market value was $50M. Since Bruker Optics' 2007 revenue was approximately $58M, (13) nearly 14% of its income came from outside of the research segment, but it was spread across many applications and industries.

2 Methodology / Approach

The first step in characterizing FT-IR spectrometer performance trends over time was to create a universal metric or benchmark. This benchmark, named P_{spec}, was a combination of industry-standard specifications applicable to all FT-IR spectrometers. The industry-standard specifications that were used to generate P_{spec} are defined below.

2.1 Spectrometer Performance Specifications

- Bandpass: This specification is the difference between the maximum and minimum frequencies in which a spectrometer can operate. This value is determined by the source, beam splitter, and detector combinations that the instrument supports and is in units of wavenumbers or cm^{-1}. (8) A spectrometer is considered to be higher performing the greater its Bandpass.
- Signal to Noise Ratio (SNR): SNR is the ratio between $Power_{Signal}$ and $Power_{Noise}$. In order for a signal to be considered a valid data point, it needs to be well above the noise floor or have a high SNR. The higher the SNR, the higher the signal quality and validity (8). SNR is unit-less.
- ADC bit resolution: An ADC or Analog to Digital Converter has a resolution range that equals $2^{(value\ in\ bits)}$. This represents the total quantized amplitude values to which an analog signal can be converted. For example, a 16 bit ADC has 2^{16} or 65,536 amplitude levels. The higher the ADC bit resolution, the more accurate analog to digital conversions will be (8). ADC bit resolution is in units of bits.
- Spectral Resolution: Spectral resolution is the minimum width over which a spectrometer can distinguish different spectral features or peaks. The general resolution limit of an instrument is the inverse of its maximum achievable optical path difference (OPD) of the interferometer which was defined in section 1.4 (7). Resolution is expressed in units of wavenumbers or cm^{-1}. A smaller value in spectral resolution reflects a higher resolution performance since narrower spectral features can be distinguished.
- Wavenumber Accuracy (WA): Wavenumber Accuracy is the difference between the wavenumber of a known reference peak and an instrument's measured wavenumber of that same peak. The smaller the value for Wavenumber Accuracy, the more accurate the spectrometer (14). Similarly to both Bandpass and Resolution, WA is expressed in units of cm^{-1}.
- Volume: There are two values of interest with respect to volume which has units of m^3. The first is by multiplying the length, width, and depth dimensions resulting in the volume of the total system and the other by subtracting the volume of just the computer processing components from the total system volume. As values of volume decrease,

spectrometer performance increases as it retains the same functionality, but requires less physical space.

- Weight: Similarly to the volume metric, there are two relevant values of weight – the total and the total minus the computer processing weight. Weight is in units of kg. As weight decreases, spectrometer performance increases because the same functionality is retained using less mass.
- Power Consumption: This is the measure of power consumed by the instrument and is in terms of kW. Spectrometer performance increases as power consumption decreases because the instrument's power use is more efficient.
- Cost: The present value (PV) of the instrument cost was calculated by taking the dollar value of the year it was available on the market and discounting appropriately using average US treasury security interest rates. The values are expressed in units of $1,000 or $K. Spectrometer performance increases as cost decreases because the same functionality is retained, but at a lower consumer cost.

2.2 Universal Performance Metric: P_{spec}

P_{spec} is composed of Bandpass, SNR, ADC bit resolution, Spectral Resolution, and Wavenumber Accuracy. Volume, weight, power consumption, and cost were also analyzed for each spectrometer system, but were not included in the P_{spec} calculation because they do not directly affect a spectrometer's functional performance. Rather, these metrics are used as effectiveness references. The initial formula for P_{spec} is displayed in the equation below.

$$Pspec = \frac{Bandpass * Signal\ to\ Noise\ Ratio * ADC\ Bit\ Resolution}{Spectral\ Resolution * Wavenumber\ Accuracy}$$

Equation 3: Original P_{spec} Formula

The rationale for placing a specification in the numerator or denominator depended on whether an increase in the specification value would increase or decrease the performance. For example, an increase to the Signal to Noise Ratio (SNR) value corresponds to an increase in SNR performance of any spectrometer making it part of the numerator of P_{spec}. An increase in

the Resolution value would result in a decrease in Resolution performance which is why it is part of the denominator.

The rationale for multiplying the values within the numerator and denominator was determined by taking the limits of the values at zero and infinity. For example, if Bandpass approaches zero, P_{spec} should approach zero because a spectrometer with zero Bandpass is useless. It follows that if Bandpass approaches infinity, P_{spec} should also approach infinity. On the other hand, if Wavenumber Accuracy approaches zero, P_{spec} should approach infinity and if Wavenumber Accuracy approaches infinity, P_{spec} should approach zero.

While the P_{spec} formula in Equation 3 theoretically represents an equally weighted combination of specifications, there is an issue of magnitudes. For example, Bandpass typically has the magnitude of 10^4, but ADC bit resolution only has a magnitude of 10^1. This would put roughly 10^3 times more weight on the Bandpass specification over the ADC bit resolution which is undesirable. In order to maintain equal weights of each individual specification's contribution to P_{spec}, they were all normalized. Bandpass, SNR, ADC bit resolution, spectral resolution, and wavenumber accuracy specifications were divided by the specification values of the first instrument commercially available. Taking normalization into consideration, the revised P_{spec} formula is shown below. From Equation 4, it follows that the value of P_{spec} for the first system analyzed is one. Any subsequent system P_{spec} value greater than one indicates an increase in performance and a P_{spec} value of less than one indicates a decrease in performance relative to the first spectrometer system released.

$$P_{spec} = \frac{\frac{Bandpass}{Bandpass_0} * \frac{SNR}{SNR_0} * \frac{ADC\ Bit\ Resolution}{ADC\ Bit\ Resolution_0}}{\frac{Spectral\ Resolution}{Spectral\ Resolution_0} * \frac{Wavenumber\ Accuracy}{Wavenumber\ Accuracy_0}}$$

Equation 4: Revised P_{spec} Formula

2.3 Design Structure Matrix Analysis

In order to determine the architectural trends of Bruker Optics' spectrometers, Design Structure Matrix (DSM) analysis was used to trace links between components within each FT-IR spectrometer system. DSM analysis is a tool that enables a compact and clear representation of

complex systems by mapping components and the relationships between them. These relationships can be further described as interfaces, interactions, and interdependencies (15). There are several types of DSMs and they are used in a wide variety of applications spanning from project management to organizational design. The type best suited for analyzing a product's system architecture, in this case an FT-IR spectrometer, is referred to as a "component-based" DSM (16).

The level of decomposition and its subsequent components determine the size of the DSM since a component-based DSM is an N by N matrix where N is the total number of components. All systems can be decomposed almost indefinitely, so a decomposition limit needed to be defined. Otherwise, the DSMs of the different spectrometers would not be comparable to each other. For the scope of this thesis, the spectrometer systems were decomposed from the top down to a maximum of two levels. An example of the levels of decomposition is shown in Figure 13 below. By limiting decomposition to the second level, the DSMs were manageable in size yet still offered sufficiently detailed architectural information.

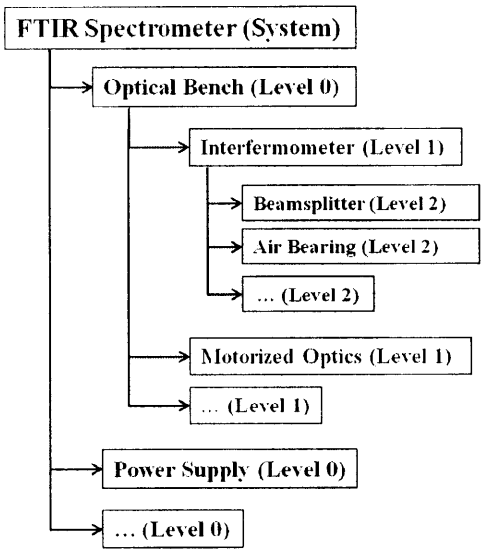

Figure 13: Levels of Decomposition

The relationships among components are often referred to as links. Defining different types of links can vary according to the system or the individual undertaking the analysis. De Weck and Magee propose there are four - matter, energy, information, and value (17). Pimmler and Eppinger define four links as well - spatial, energy, information, and materials (18). For the

purposes of this thesis, a combination of the two previous definitions was used to differentiate the links in FT-IR spectrometer DSMs. They are listed below along with a brief description:

- Material/Spatial – These links represent either a required orientation or a physical connection between or among two or more components. In the case of an FT-IR spectrometer, mirrors exhibit spatial links because their alignment or orientation is critical to the system functionality. Material links manifested themselves as wiring, screws, bolts, epoxy, or any other connective material. Material/Spatial links were indicated by "1" in the DSMs.
- Energy – These links represent the flow of energy. In the case of FT-IR spectrometers, these links were flows of electricity or IR radiation. Energy links were marked by "2" in the DSMs.
- Informational – These links represent the flow of information among components. Information links are similar to energy links for electronic components, but the differentiator between them is that information links are the transfer of digital signals. These links were marked by "3" in the DSMs.

These links are directional from the components of the rows to the components in the columns. This directionality results in asymmetric DSMs. To help visualize the component-based DSM, Figure 14 below is an example with all three types of links.

	A	B	C	D
A		1		1
B	1		3	2
C				
D	1	3		

Figure 14: Example DSM

There are four components A, B, C, and D in this simple system. There are material/spatial links from Component A to both B and D. Component B has a material/spatial link to A, but also an information link to C and an energy link to D. Component C has no links to any other component while Component D has a material/spatial link to A and also an informational link to B.

All data recording and analysis was executed using either Microsoft Excel or MATLAB and the data flow is shown in Figure 15 below. The items in black are Excel files and the items in blue are MATLAB files. Both Excel and MATLAB were used due to the author's personal familiarity with the software.

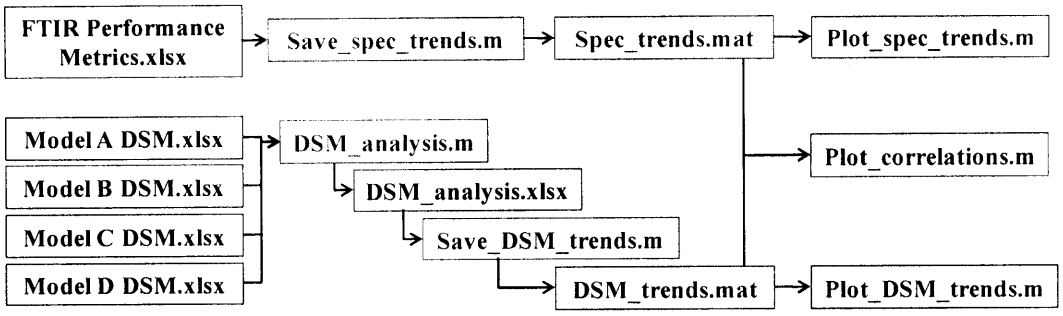

Figure 15: P_{spec} and DSM Analysis Data Flow

Excel was a natural choice to construct the DSMs and it was also used to record the P_{spec}, volume, weight, power consumption, and cost metrics. Once the performance metrics and DSM spreadsheets were created, the data was analyzed with MATLAB scripts and saved as .mat files. Using these .mat files, all analysis plots were generated by additional MATLAB scripts. All the files displayed in Figure 15 can be found in section 7.4 the Appendix.

3 Results

Four Bruker Optics FT-IR spectrometers were examined using the P_{spec} benchmark and DSM analysis. These four specific spectrometer models were chosen for two reasons. The first reason was that they spanned across Bruker Optics' product offering from 1976 to 2008. The second reason was that they represented the highest specified performance spectrometers on the market, and therefore gave an accurate representation of the maximum performance increases for all FT-IR spectroscopy during this period. The four systems have been labeled Model A, B, C, and D. Models A, B, C, D were available to the consumer market in 1976, 1985, 1988, and 2008 respectively.

3.1 Performance Results

The following section displays the plots of P_{spec}, volume, weight, density, power consumption, and cost of all four spectrometer models. Note for the weight, volume, and resultant instrument density, there are two overlaid plots which represent the inclusion and exclusion of computing components. For power consumption and cost, a separate plot excluding computing components could not be determined as the data was not available and could not be approximated or deduced. This issue will be discussed in more detail in section 3.1.3.

Computer components were common among the spectrometer systems and were a subset of: data console, processing unit, personal computer, display, plotter, keyboard, and mouse. Models A and B included data console, processing unit, display, plotter, and keyboard. As computer technology advanced over the years, Models C and D included a personal computer which was essentially the merging of a data console and processing unit. A mouse was also added as a computing component. The display and keyboard components remained consistent over the years.

3.1.1 P_{spec}

Figure 16 below displays both P_{spec} and $\ln(P_{spec})$ versus time. From observation, there was ambiguity in determining the proper fit that accurately quantified P_{spec} as a function of time.

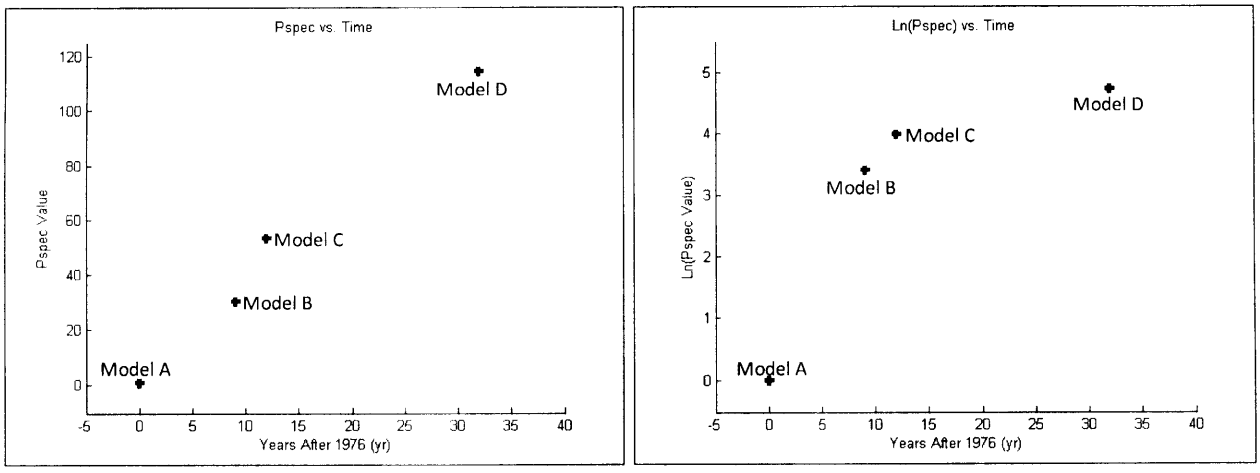

Figure 16: Spectrometer P_{spec} Trends (10)

The first approach was to approximate a linear fit using all four data points. Using MATLAB's curve fitting tool, cftool.m, a linear fit was found to be Equation 5 below.

$$P_{spec}(t) = 3.542t + 2.804$$
$$with\ R^2_{fit} = 0.9802$$

Equation 5: P_{spec} Linear Fit for Models A, B, C, and D

This linear fit implied that the rate of P_{spec} increase to be approximately 3.5% per year and it eliminated any potential resemblance to an "S" curve (19). It also implied unlimited future increase which was not realistic. P_{spec} limitations are discussed further in section 4.1.

The second approach was to view the first three data points separately from the last one. For the first three systems, Models A, B, and C, there appeared to be an exponential increase in P_{spec}. This exponential relationship was evident in the approximately linear relationship of the first three $\ln(P_{spec})$ points. The exponential fit of the first three systems was found to be Equation 6 below.

$$P_{spec} = 4.1 \times e^{0.215t} \qquad for\ all\ t \leq 12$$
$$with\ R^2_{fit} = 0.9807$$

Equation 6: P_{spec} Curve Fit for Models A, B, and C

This exponential fit implied that P_{spec} would reach the P_{spec} value of Model D in nearly fifteen and a half years after 1976 or by mid 1991. This was clearly not the case for P_{spec}. Soon after Model C's release to the market, P_{spec}'s rate of increase reduced drastically. Exactly when this reduction occurred and its magnitude was ambiguous. Without an additional P_{spec} data point for $t > 12$ and $t \leq 32$, a future projection of P_{spec} cannot be accurately estimated by comparing to Model D's P_{spec} value. Unfortunately, Bruker did not produce another research-grade model in this timeframe so this piece-wise approach to P_{spec} fitting could not be verified. Of the two curve fits above, the more reasonable approximation of P_{spec} seemed to be the exponential increase for models A, B, and C followed by a reduction in the rate of increase for model D because this piecewise approach was consistent with the trends in volume, weight, and cost.

3.1.2 Volume, Weight, and Density Trends

As can be seen in next three figures, computer components historically played a significant role in a spectrometer system's volume, weight, and resultant density. In Figure 17, for Models A and B, the volumes of the computer components were over a cubic meter, whereas for Models C and D, the computer component volume was near zero.

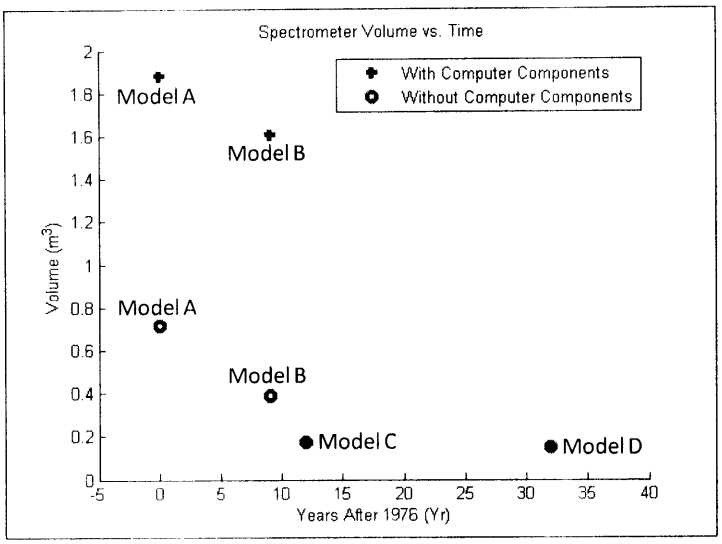

Figure 17: Spectrometer Volume Trend (10)

This was consistent with the emergence of personal computers (PC)s in the early 1970's (20). Spectrometer systems built prior to the 1980's had data processing and user interface components that were highly integrated with the spectrometer's optics. Since the early 1980's, the data processing and user interaction interface components were decoupled from the system's optics when modularized into a PC component.

What was interesting to note was that the system volume decreased by over a factor of four within the first 12 years independently of the computing components. It has remained relatively unchanged since with only a reduction of 0.02 m^3 over the last twenty years. This decrease in volume resulted in P_{spec}/volume trends shown in Figure 18 below.

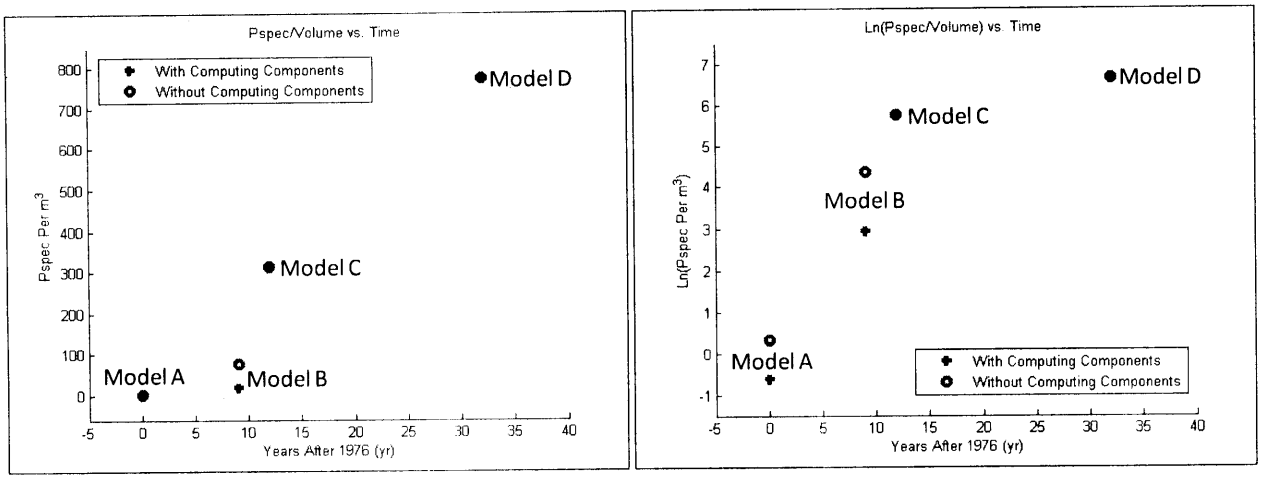

Figure 18: P_{spec} / Volume Trend (10)

Similarly to the P_{spec} plot, there appeared to be an exponential increase of P_{spec}/volume for the first three systems which was noticeable in the linear relationship of models A, B, and C in the logarithmic plot.

Unlike volume, spectrometer weight without computer components, show in Figure 19, has not changed much over the entire history of Bruker Optics.

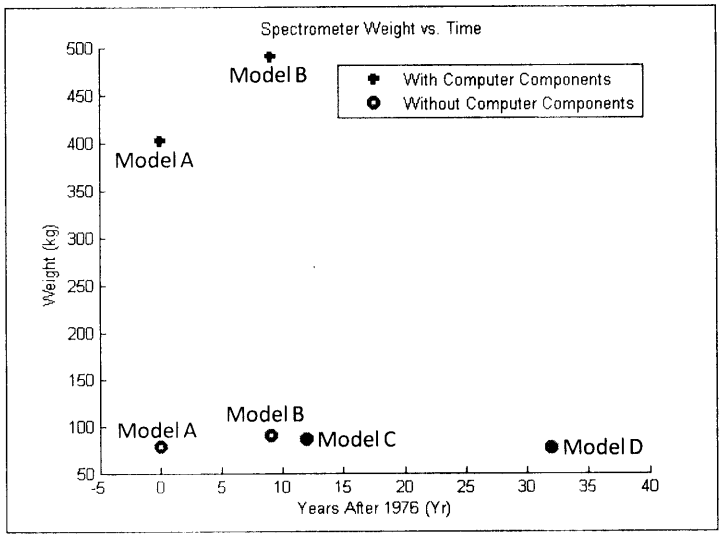

Figure 19: Spectrometer Weight Trends (10)

The computer components for Models A and B weighed more than five times the optical components which indicated the incredible progress in these components in this timeframe. Model C saw a dramatic reduction of over 400 kg to 86 kg and Model D's weight was further reduced by another 10 kg. Since Model B in 1985, subsequent spectrometer weights have

decreased at a rate of nearly 0.6 kg/year. It follows from the decreasing volume trend and the relatively unchanging weight trend that spectrometer density, shown in Figure 20 below, would increase.

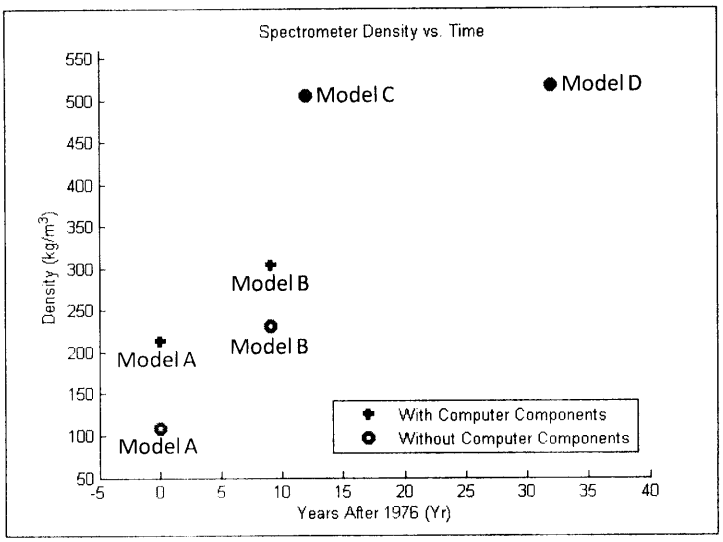

Figure 20: Spectrometer Density Trends (10)

What was surprising was the rate of density increase. Even with computer components, density increased by a factor of nearly two and a half during the first 12 years. More importantly, density without computer components increased by nearly a factor of five over the same time period. Over the last 20 years, the density rate decreased to an incremental increasing rate of approximately 0.81 kg/cm^3 per year.

The dramatic increase in spectrometer density over Models A, B, and C was not expected. Prior to the analysis, it was thought that reduction of computer component weight and volume would leave system density relatively consistent and unchanged. Figure 20 clearly shows that this was not the case. Rather, this spectrometer density increase must be attributable to factors other than just computer components' density increases.

3.1.3 Power Consumption and Cost Trends

Unfortunately, computer component power consumption could not be broken out from the entire spectrometer system's power consumption because the information was unavailable and

could not be accurately calculated. Figure 21 below displays spectrometer power consumption over time.

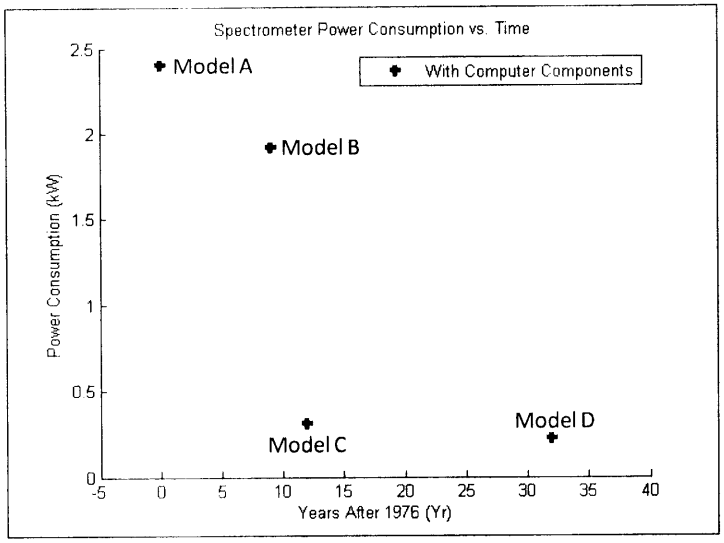

Figure 21: Power Consumption Trend (10)

Between Models A and B there was a reduction of approximately 20% from 2.4 kW to 1.92 kW, but between Models B and C, there was a reduction of over 80% from 1.92 kW to 310 W. Power consumption's decreasing rate has since slowed down to roughly 5 W/Yr.

Like power consumption, computer component cost could not be separated from the entire system cost. Figure 22 below displays the present value (PV) cost in 2009 dollars of all four spectrometer models. The discount rates used to calculate each model's PV was the average nominal United States treasury constant maturity interest rates which can be found in Table 10 in the Appendix.

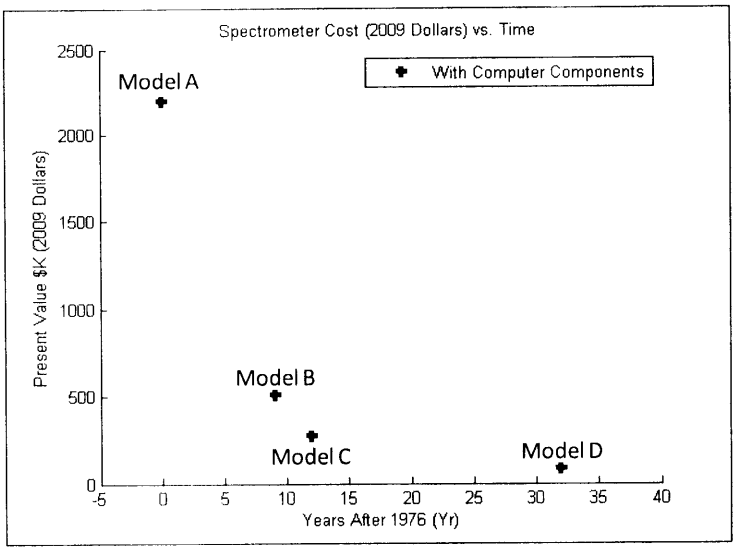

Figure 22: Spectrometer Cost Trend (10)

There was a clear exponentially decreasing trend in PV cost of spectrometer models over time. The exponential fit was found to be Equation 7 below and is a good approximation of the cost of Bruker Optics' future research-grade spectrometers.

$$PV_{Spectrometer}\ (t) = 2195e^{-0.1655t}$$

$$with\ R^2_{fit} = 0.9967$$

Equation 7: Spectrometer Cost Exponential Fit

Even though the rate of cost decrease slowed to rate of approximately $480 per year, Bruker Optics delivered greater performance per dollar with each new model release which is evident in Figure 23 below.

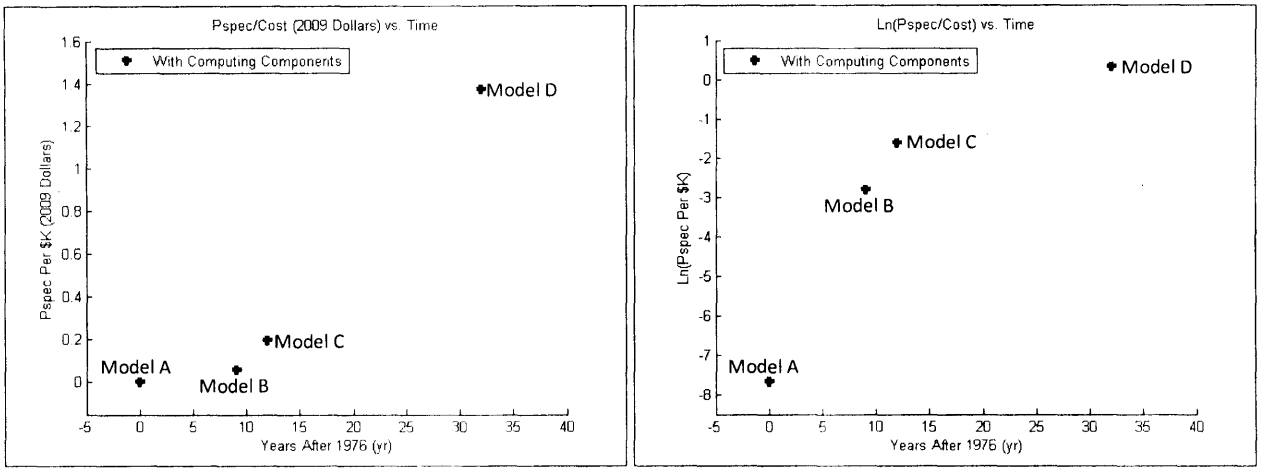

Figure 23: P_{spec} / Cost Trend (10)

From models A to B, there was only a slight increase in P_{spec} per $K, but among models B, C, and D, there was a noticeable increase from 0.0590 per $K to 1.3737 per $K. As with the other trends that involved P_{spec}, there was curve fitting ambiguity. The plot on the left of Figure 23 displays a linear relationship between the last three models. Whereas the logarithmic plot on the right displays an exponential relationship between models A, B, and C. A linear curve fit of these last three points and an exponential fit of the first three data points resulted in Equation 8 and Equation 9 respectively.

$$\frac{P_{spec}}{Cost}(t) = 0.05782x - 0.479 \quad for\ all\ t \geq 9$$

$$with\ R^2_{fit} = 0.9986$$

Equation 8: P_{spec} / Cost Linear Fit

$$\frac{P_{spec}}{Cost}(t) = 0.00164e^{0.398t} \quad for\ all\ t \leq 12$$

$$with\ R^2_{fit} = 0.9999$$

Equation 9: P_{spec} / Cost Exponential Fit

3.2 Design Structure Matrix Analysis

3.2.1 General Observations

When the DSMs for the four models were created, it became clear that the links between components followed a distinct pattern. While many matter/spatial links existed independently of energy and informational links, the opposite was never the case. All energy and informational links always coincided with a matter/spatial link. This was because energy and information had to flow through or across a physical or spatial link. For example digitized voltage readings from a spectrometer's ADC (informational link) flowed through wiring (physical links) to the computer processing components. Another example would be IR radiation (energy link) flowing across adjacent mirrors (spatial link). Because of this pattern, the link categories in Section 2.3 were adjusted to those shown in the Figure 24 below. The link definitions remained the same.

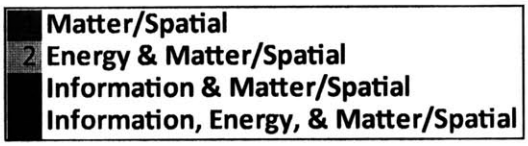

Figure 24: Adjusted DSM Link Types

There was an additional fourth link type which was a combination of all three types. All link types were color-coded to aid identification when viewing the DSMs since numbers were not easily observable.

The four color-coded DSMs can be found in section 7.2.2 in the Appendix. Because the DSMs were created through direct observation of the spectrometer models, the components were clustered by physical proximity or functional commonality. Examples of clustering by physical proximity were the Sample Compartment and Detector Compartment Subsystems in models A and B. The components in these clusters were physically located close to each other and shared matter/spatial links. An example of clustering by functional commonality was the Air Subsystem found in all four DSMs. The Air Subsystem components lacked physical proximity as they were

located across the entire spectrometer, but still had the common functionality of providing the system with pressurized air.

Although no two DSMs contained exactly the same components, there was enough commonality that the component order along the axis of all four DMSs was very consistent. This component order consistency enabled clustering consistency as well as reliable analysis. The next section highlights the part count, matter/spatial link, energy link, and informational link trends. In contrast to the spectrometer performance trends, the impact of computer components on the spectrometers' architectural trends was minimal. The contribution from computer components emerged as a consistent offset because they were architecturally consistent across all models as mentioned earlier in section 3.1.

With the exception of model D's component count and informational link count, all other DSM data exhibited continuous decreases over time. Since the spectrometers were increasing in performance over the same time frame, these performance gains were accompanied by simpler design.

3.2.2 DSM Trends

Figure 25 below displays the component counts of the DSMs of all four models.

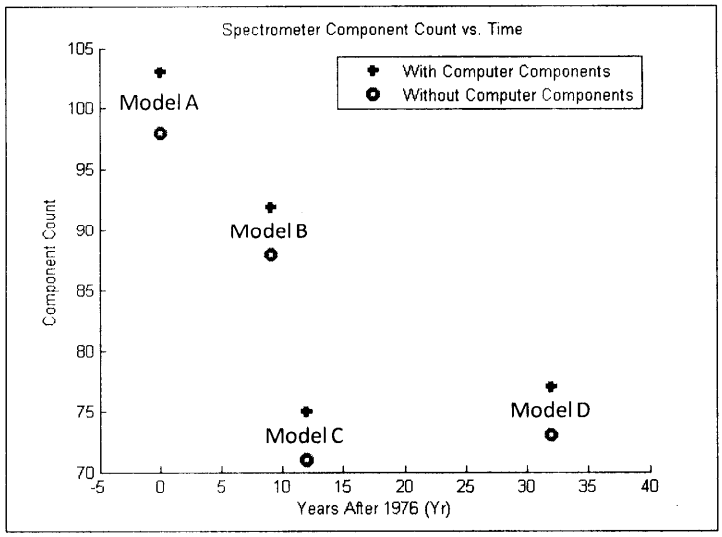

Figure 25: Spectrometer Part Count Trend (10)

There was a decrease from 103 to 92 components which was an average rate of 1.2 components per year between models A and B, but there was a greater decrease of over 17 components in the three years between models B and C. Then in the 20 years between models C and D, there is a slight increase from 75 to 77 components. This increase in component count for model D was unexpected as it was thought that component count would continuously decrease over time.

Figure 26 below exhibits the number of matter/spatial links per instrument over time. Again, the computer components offset is visible but did not affect the overall trend.

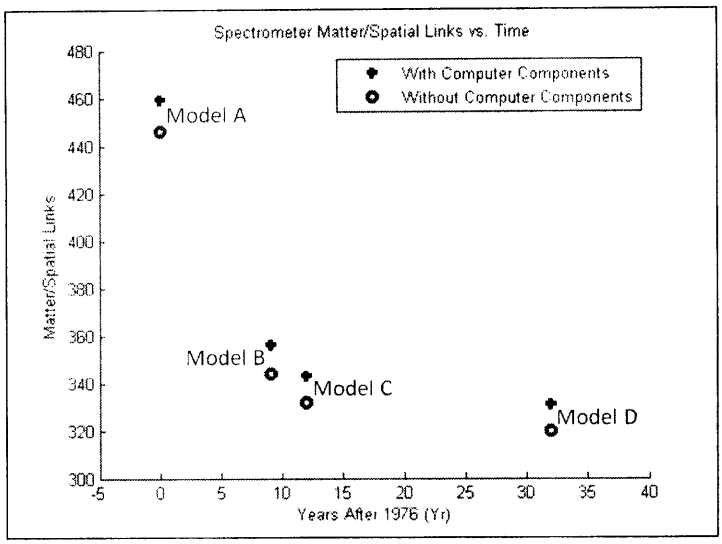

Figure 26: Spectrometer Matter/Spatial Link Trend (10)

There was a sizeable reduction of over 100 matter/spatial links or just over 11.4 links per year between models A and B. This decreasing rate slowed to a little over 4.3 links per year between models B and C and leveled out to an incrementally decreasing rate of 0.6 links per year between models C and D. By observation, the matter/spatial link data looks very similar to the cost data in section 3.1.3 which will be explored in more detail in section 4.2.

Similarly to the matter/spatial link data, the number of energy links over time shown in Figure 27 below was continuously decreasing, but at very different rates between each spectrometer model.

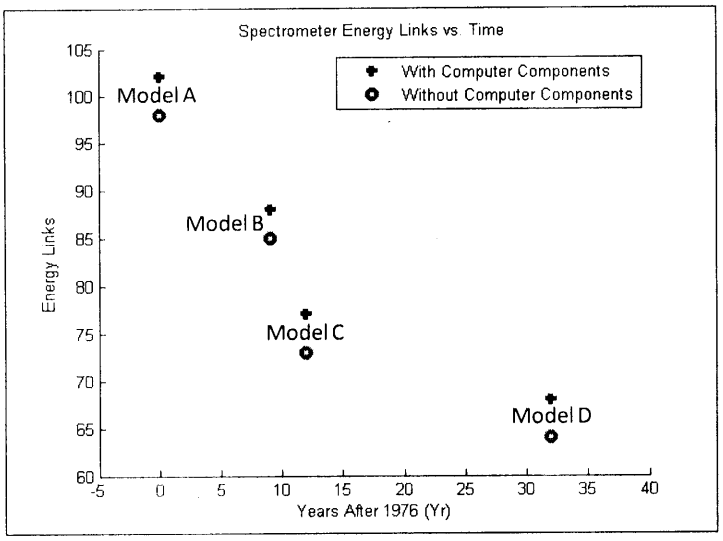

Figure 27: Spectrometer Energy Link Trend (10)

Between models A and B, there was an average decreasing rate of over 1.5 links per year followed by a greater rate decrease of over 3.6 links per year between model C and D. Over the last 20 years, the decreasing rate has slowed to less than a half a link per year.

Figure 28 below shows the number of informational links across all four instrument models. Between models C and D, the informational link data clearly behaves similarly to the component count plot in Figure 25.

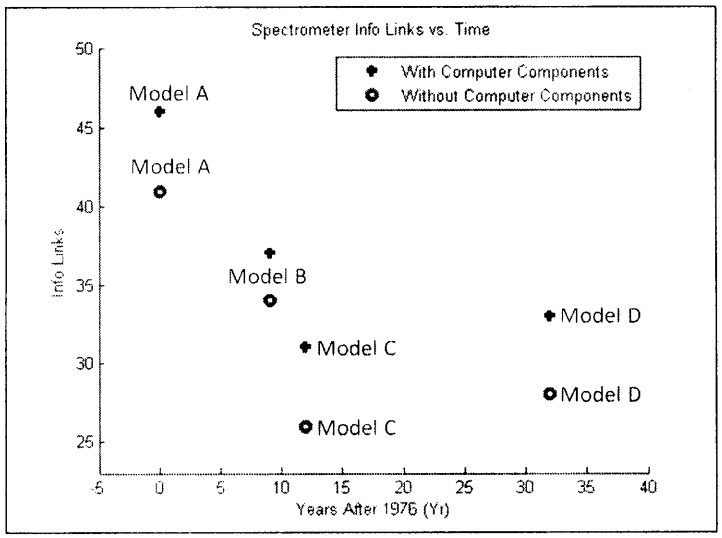

Figure 28: Spectrometer Informational Link Trend (10)

When explored in greater detail, the increased part count in model D was found to be due to the increased number of informational links. The other types of links, matter/spatial and energy, had

continuously decreased over time as seen in Figure 26 and Figure 27 respectively. This only left informational links responsible for the increased part count found in model D.

4 Interpretation / Discussion

4.1 Performance [P_{spec}]

After exhaustively comparing the performance and DSM architectural data of the four models, no clear correlations were found between P_{spec} and DSM architectural trends. (Please refer the Appendix for the detailed data.) While this was disappointing, it was not unexpected. A closer examination of the factors that contributed to P_{spec}'s increase over time was due to individual components' performance increases rather than architectural or overall design changes. From an architectural point of view, the FT-IR spectrometer has not changed much over its 30 year history. The vast majority of components were common between all four spectrometer models. Table 4 in the Appendix shows that the increases in P_{spec} were due to increases in bandpass, SNR, and ADC bit resolution performance.

Spectral resolution values actually increased from 0.04 cm-1 for model A to 0.07 cm-1 for model D which represented an overall performance decrease. Wavenumber accuracy (WA) performance remained constant at 0.01 cm^{-1} across all four systems. This would suggest that either WA performance had already reached its maximum performance limit or it was simply at a high enough performance level for the consumer market that it could be traded off for other desirable performance factors.

Bandpass increases were due to the availability of the appropriate sources, beam splitters, and detectors. From model B onward, the Bandpass metrics was at the maximum value of 49,999 cm^{-1}. The increase was in the NIR / visible spectrum range between 10,000 and 15,000 cm^{-1}. Models B, C, and D not only covered the entire IR spectrum, but also part of the visible spectrum as well.

From the definition of SNR, higher performance was achieved by either increasing $Power_{signal}$ or reducing $Power_{noise}$. Of all the industry standard performance specifications, SNR was the only one that could be potentially linked to architectural changes. Theoretically, the smaller the number of energy interfaces, the less power is lost throughout the system. For

example, gold coated mirrors reflect 97% to 99% or incident IR radiation so for each mirror along the IR radiation beam path, there was up to a 3% loss in IR signal power (21). From Figure 27 of the DSM analysis, one can see that energy links decreased from 102 to 68 across all spectrometer models which most likely would have contributed to increased IR signal throughput, or $Power_{signal}$. It follows that this $Power_{signal}$ increase would result in SNR increase.

Spectrometer ADC bit resolution performance increases were due to improved commercially available ADC technology. Table 4 shows that ADC bit resolution started at 12 bits in model A, increased to 16 bits for models B and C, and then increased again to 24 bits for model D. Bruker Optics' spectrometers had continuously integrated the highest commercially available ADC bit resolution with each new spectrometer model (22).

Although there were no observed interdependencies between P_{spec} and DSM data sets, some correlations were discovered between instrument volume, power consumption, and cost when compared to DSM data.

4.2 Volume, Power Consumption, and Cost

One might argue that the spectrometer models' volume, weight, power consumption, and cost reductions were mainly due to technological advancements in the models' computer components. This assertion was only true for weight which was already shown in Figure 19 in section 0 where the majority of the weight of models A and B was due to computer components. By removing the computer component contributions, spectrometer weight remained fairly constant across all models. This consistent weight over time was explainable due to weight's role in isolating the spectrometer from environmental vibration noise. The average weight of the four models was just over 82.5 kg which provided good vibration isolation while still allowing for manual portability.

Comparing the volume and cost trends with DSM architectural data revealed correlations between volume and component count, and cost and matter links. Figure 29 below displays the relationship between instrument volume and component count.

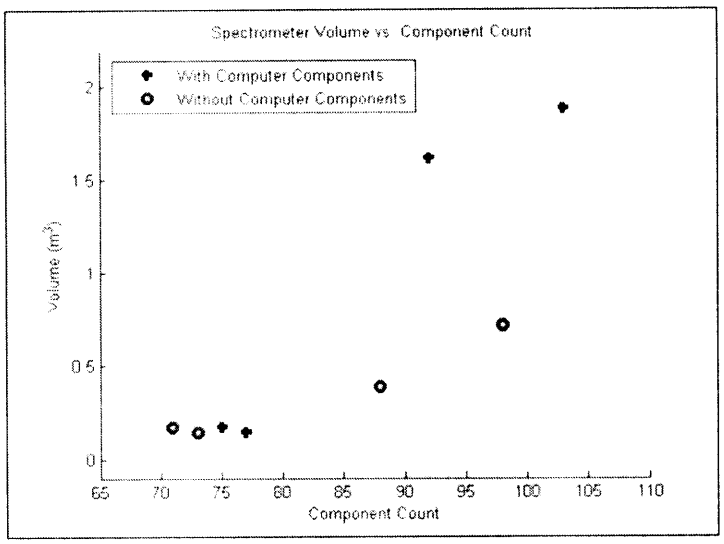

Figure 29: Spectrometer Volume vs. Component Count (10)

While neither data set, with or without computer components, displayed an indisputable trend, both did show an approximate linear relationship. Equation 10 below contains the linear fits with x as the variable for component count.

$$Volume(x) = 0.06778x - 4.928$$
$$with\ R^2_{fit} = 0.9164$$
$$Volume(x_{w/out\ computer}) = 0.02018x_{w/out\ computer} - 1.308$$
$$with\ R^2_{fit} = 0.9224$$

Equation 10: Volume vs. Component Count Linear Fits

As expected, the linear fit of the data including computer components had a slope that was over three times greater than the linear fit of the data without computer components. This was consistent with the fact that the majority of the volume of models A and B was due to computer components.

Since informational and energy links represented electrical flows, it made sense to plot system power consumption as a function of combined energy and informational link count. Similarly to volume versus component count, power consumption versus combined energy and informational link count, shown in Figure 30 below, could only be approximated as linear.

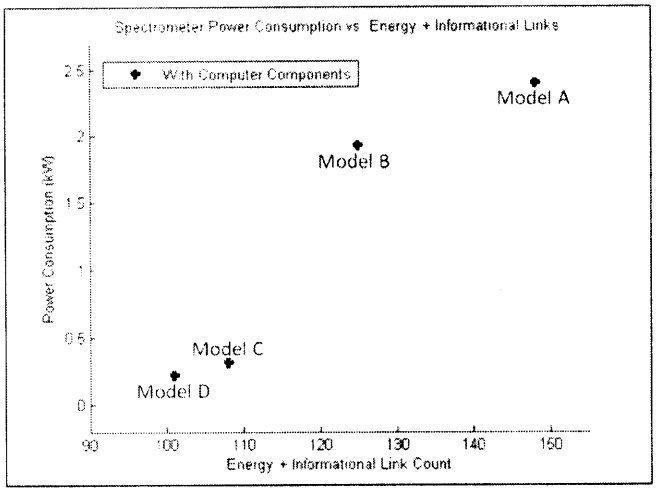

Figure 30: Spectrometer Power Consumption vs. Energy + Info Link Count (10)

There was an obvious trend that power consumption increases as combined energy and info link count increases, but Equation 11 below is a linear fit of the data with x representing combined energy and informational link count. As can be seen by the low R_{fit}^2 value, this linear fit is only an approximation.

$$Power\ Consumption(x) = 0.005063x - 4.888$$
$$with\ R_{fit}^2 = 0.8606$$

Equation 11: Power Consumption vs. Energy + Info Link Count Linear Fit

Unlike the trend of power consumption versus combined energy and informational link count, which could only be approximated as linear, cost versus matter/spatial link count, shown in Figure 31 below, was convincingly linear.

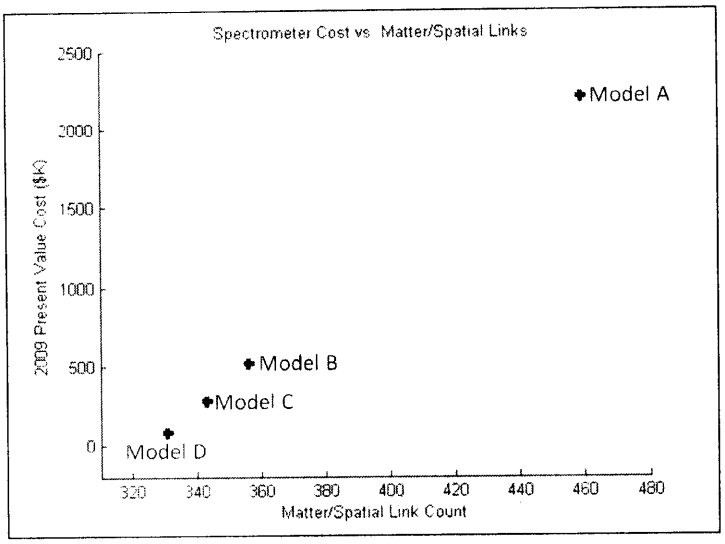

Figure 31: Spectrometer Cost vs. Matter/Spatial Link Count (10)

Equation 12 below is the linear fit for cost versus matter/spatial link count with x representing matter/spatial link count.

$$Cost(x) = 16.49x - 5373$$

$$with\ R^2_{fit} = 0.9999$$

Equation 12: Cost vs. Matter/Spatial Link Fit

This is a very important correlation because it could be used to predict future spectrometer costs relative to changes in the matter/spatial links of the spectrometer's architecture. As mentioned earlier in section 2.3, matter links were defined as wiring, screws, bolts, epoxy, or any other connective material and spatial links were defined as required orientation between components. All matter/spatial links have an associated cost whether it be manufacturing or machining cost, so a correlation between the number of matter/spatial links and instrument cost was expected. However, it was surprising how perfectly linear this correlation was.

5 Strategic Recommendations

5.1 Architectural Strategy

5.1.1 Performance [P_{spec}]

With the exception of energy link count's potential influence on SNR, architectural changes in general did not affect performance as measured by P_{spec}. However, it is still very important to discuss future values of P_{spec} as it is an indicator for the technological future of the entire FT-IR spectroscopy industry. When looking back at Figure 16, model C was a successful, market-leading product for nearly 20 years and was only recently replaced by model D in 2008. The longevity of model C implies that a P_{spec} value of over 53 already met or exceeded consumer performance expectations during that time period. This also implies Model D's P_{spec} value of over 114 may be unnecessarily high. Any future increases in P_{spec} will be due to increases in spectral resolution, SNR, or ADC bit resolution. The other two contributors to P_{spec}, Bandpass and Wavenumber Accuracy, have already reached their maximum value with models B and beyond. Spectral resolution, ADC bit resolution, and SNR are theoretically limitless.

Even though P_{spec} has the potential to increase indefinitely, the spectrometer consumer market will determine whether P_{spec} is "good" enough at its current value of 114. Through personal knowledge of the industry, the author asserts that except for the most demanding research applications, a P_{spec} value of 114 will meet research consumers' performance expectations for the next 15 years.

5.1.2 Volume, Power Consumption, and Cost

The analysis in the section 4.2 points to some obvious architectural strategies that Bruker Optics should continue to pursue in order to further reduce instrument volume, power consumption, and cost. Except for model D, Bruker Optics has been steadily reducing component count and should continue to do so with their future model releases which will reduce instrument volume.

The same approach applies to power consumption. Although power consumption may have been historically a low priority to consumers and spectrometer firms, with the recent cultural emphasis in environmentally friendly products, decreased power consumption will help build

Bruker Optics' "green" company image and brand equity. Future power consumption reductions can be achieved by further reductions in energy and informational links in the instruments' architecture.

Matter/spatial link count reduction is probably the most important architectural strategy that Bruker Optics should continue to pursue. As spectrometer costs continue to decrease exponentially, Bruker Optics must reduce manufacturing costs at the same rate to maintain the same profit margins. If they cannot match the decrease, they will continually make less profit per spectrometer sold.

5.2 Marketing Strategy

As FT-IR spectrometer prices continue to exponentially decrease, research-grade systems will become more and more commoditized. This continued commoditization, low barrier of entry for competition, and incremental growth in the research segment jeopardizes Bruker Optics' future growth prospects. Price sensitive consumers may switch to cheaper systems offered by competitors. If Bruker Optics hopes to ensure future revenue growth, they may have to capture greater market share by targeting other market segments.

5.2.1 Segmentation

Prior to targeting, complete market segmentation needed to be established. Because most available marketing data was organized into separate NIR from the MIR/FIR markets, this division is reflected in the following marketing analysis. Figure 32 and Figure 33 below display the NIR and IR spectroscopy market segmented by product. Unlike the market data in section 1.6, which was segmented by application, function, and region, the data below was segmented by product because it reflected common consumer needs.

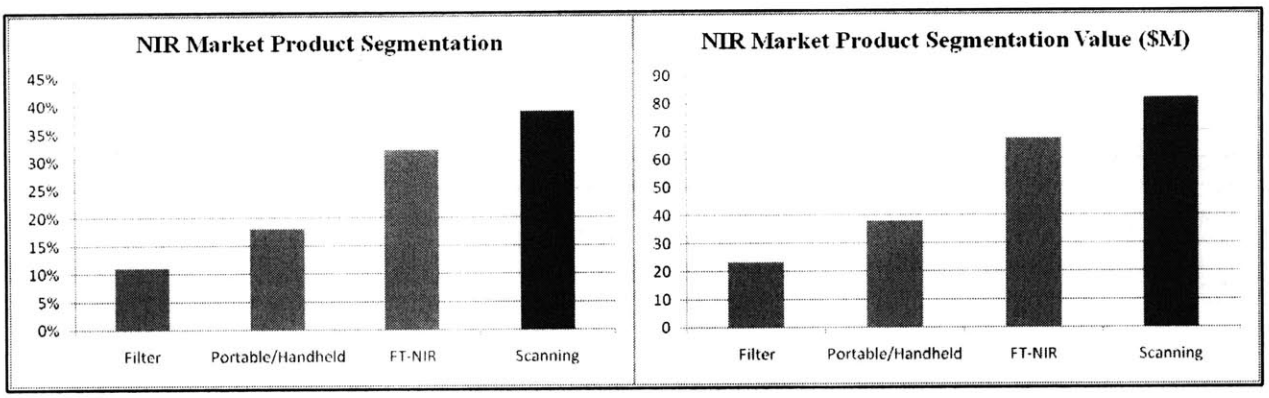

Figure 32: NIR Market Product Segmentation (13)

Of all these NIR systems, nearly 70% of the products utilize dispersive technology which is represented in the Filter, Portable/Handheld, and Scanning segments. This is because FT-NIR spectrometers are not small enough for portable uses or are not price competitive enough to drive adoption over Filter and Scanning spectrometers at the current time. However, the data collection speed and quality advantages of FT-NIR are gradually replacing Filter and Scanning technologies with a projected compounded growth rate (CGR) of approximately 6% from 2007 to 2012. The fastest growing product segment is Portable/Handheld with a projected CGR of nearly 14% from 2007 to 2012 (13).

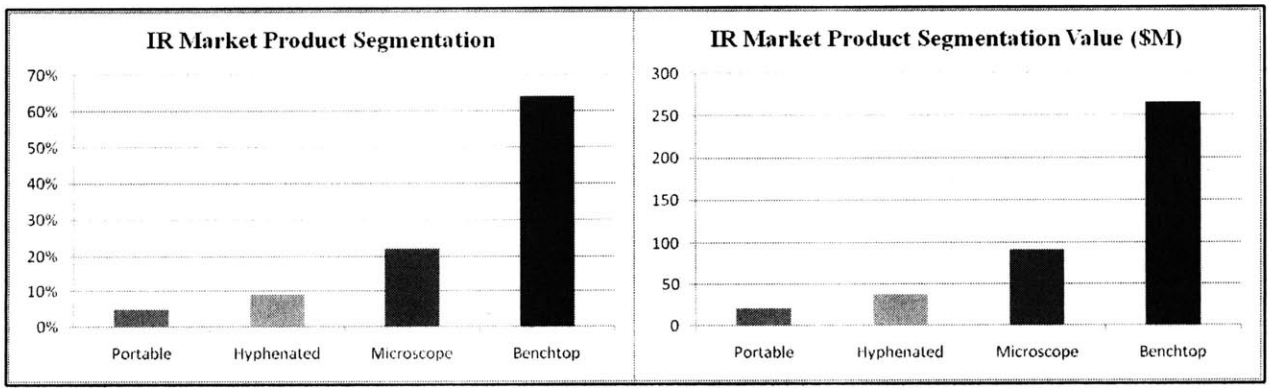

Figure 33: IR Market Product Segmentation (13)

Benchtop and Microscope systems make up over 80% of the total IR market. Similarly to the NIR market, the portable product segment is experiencing the greatest growth with a projected CGR of 24% from 2007 to 2012 (13). While both NIR and IR markets were similar in applications and functions, when it came to consumer behavior and perceptions, they shared few

commonalities, but many differences according to SDI Inc's spectrometer end-user survey in 2008.

5.2.2 Consumer Behavior / Perceptions

The only commonality between the NIR and IR consumer behavior was in regard to vendor selection criteria. NIR consumers named performance, specifications, and service as the top three influences. MIR consumers named the same three influences, but in a different order - performance, service, and specifications. Both consumer groups also indicated that recommendations were the least influential in determining a vendor (23).

Table 3 below displays the behavioral and perceptual differences between the two consumer markets.

Differences	NIR	IR
Spectrometer Useful Lifecycle	58% ≤ 8 Years	47% ≤ 8 Years
Age of Existing Spectrometer	35% ≥ 8 Years	44% ≥ 8 Years
Recent Spectrometer Purchase Price	50% ≥ $50K, 24% ≥ $75K	38% ≥ $50K, 16% ≥ $75K
Technology	Majority Dispersive (Scanning)	Majority FT-IR
Brand Preference	32% (Industry Leader)	17% (Third)
Brand Loyalty	Low (28% No Preference)	Medium (20% No Preference)
Vendor Rating	7.5 (Industry Leader)	7.3 (Second)
Vendor Satisfaction	8.2 (Industry Leader)	7.5 (Second)

Table 3: Consumer Differences between NIR and IR Markets (23)

The most telling differences between NIR and IR consumers were in technology, price sensitivity, brand preference and loyalty, and vendor ratings. As mentioned in section 5.2.1, the majority of NIR products utilized dispersive technology, not FT-IR; whereas nearly all of the IR products utilized FT-IR.

NIR consumers were less price sensitive which was evident in recent spectrometer purchase prices and vendor price ratings. Recent NIR spectrometer purchases were nearly 10% greater in price categories of over $50K and over $75K than IR spectrometer purchases. While NIR consumers scored Bruker Optics lowest in satisfaction of price, they also scored price lowest in importance (23).

When it came to brand preference and loyalty, nearly 30% of NIR consumers did not have a brand preference which implied low brand loyalty. Of those who did state a preference, 32% of

them chose Bruker Optics who was the industry leader by 7% over Thermo Scientific. IR consumers exhibited a higher brand loyalty with only 20% not stating a brand preference. For brand preference, Bruker Optics scored a distant third behind PerkinElmer and Thermo whose scores was 40% and 35% respectively (23).

Bruker Optics was the industry leader in both vendor rating and satisfaction according to NIR consumers. What was remarkable was their satisfaction rating. It was nearly a full point above the next competitor, Thermo Scientific at 7.3. Bruker Optics scored extremely high in satisfaction for pre-sale support, innovation, and instrument quality which were also the three highest important factors for NIR consumers. As stated earlier in this section, price scored the lowest in satisfaction, but also lowest in importance implying low price sensitivity. Bruker Optics was not as dominant in IR consumer ratings, but still was ranked second in overall rating and satisfaction behind Thermo Scientific whose rating and satisfaction was 7.7 and 7.9 respectively. Bruker Optics' IR consumers viewed post-sale support, instrument quality, and part/accessory availability as the top three important factors, but only scored instrument quality highly in satisfaction. Price was also rated as average importance, but scored very low in satisfaction which indicated higher price sensitivity (23).

5.2.3 Targeting

From the analysis in section 5.2.2 above, it is clear that Bruker Optics should focus on the NIR segment because of its technology transition from dispersive to FT-IR, low consumer price sensitivity, low consumer brand loyalty, and high brand preference. FT-IR technology is and will continue to replace dispersive (scanning) technology. Low price sensitivity will allow Bruker Optics to charge high prices and maintain high margins for its spectrometers. NIR consumers are also impressionable due to their low brand loyalty and are therefore easier to convince to choose Bruker Optics especially with its stellar vendor and satisfaction ratings, and industry leading brand preference percentage.

At $210M, the entire NIR market is most likely too diverse for Bruker Optics to pursue so they should also target a specific NIR sub-segment. Of the product sub-segments in Figure 32, the portable/handheld sub-segment would be the ideal choice because of its value of $38M and high CGR of 14% (13). It also presents Bruker Optics the opportunity to disrupt the current

competition in NIR handheld technology. The majority of current handheld products utilize fixed filter technology so a hand-held FT-NIR product presents a dramatic performance increase. However, Polychromix and Axsun, companies that specialize in portable instrumentation have already released handheld NIR products using MEMS technology.[3]

Because Bruker Optics cannot compete in MEMS technology, they should target the scanning sub-segment with a lower cost FT-NIR spectrometer to compete with the current low cost scanning spectrometers. This competing FT-NIR instrument should be sold at a higher price point than the existing scanning spectrometers because they offer a significant increase in performance.

6 Conclusion

Bruker Optics has historically catered to researchers by producing FT-IR spectrometers of the highest performance specifications. As a result, they have retained dominant market share in the IR research segment. With a P_{spec} value of 114, Bruker Optics' latest research-grade spectrometer may offer more performance than what consumers currently want or need. To combat the exponentially decreasing cost of spectrometers, Bruker Optics needs to focus on further reducing matter/spatial link count. If consumers demand smaller, more power efficient instruments, Bruker Optics must also further reduce the number of parts, energy links, and informational links within their spectrometers.

As for growth opportunities, Bruker Optics should look to target the NIR scanner sub-segment with a price-competitive FT-NIR system. With Bruker Optics' stellar vendor and satisfaction ratings and NIR consumers' low brand loyalty, they should be able to steadily convert NIR scanning consumers to adopt their FT-NIR instruments. This targeting approach will also serve to focus Bruker Optics' product development, sales, and service teams. Instead of capturing small market share across many product segments, applications, and functions, they can concentrate on capturing large market share in one specific NIR sub-segment and eliminate the risk of spreading their resources too thinly.

[3] (27), (28)

7 Appendix

7.1 Additional Reference Plots

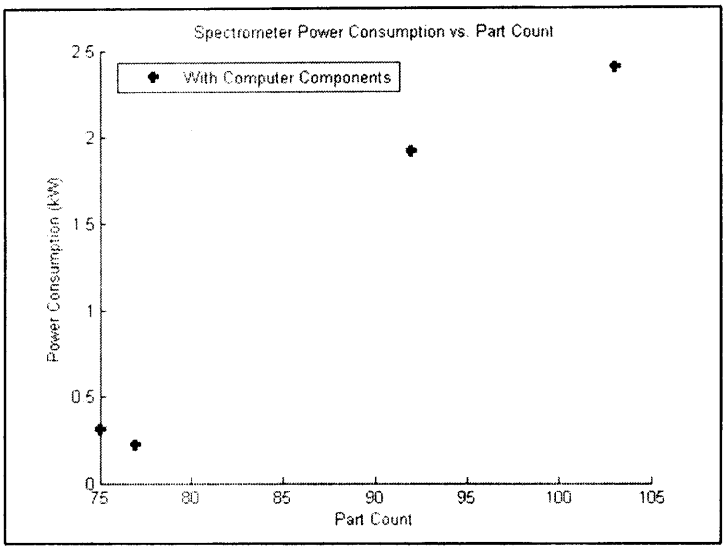

Figure 34: Spectrometer Power Consumption vs. Part Count (10)

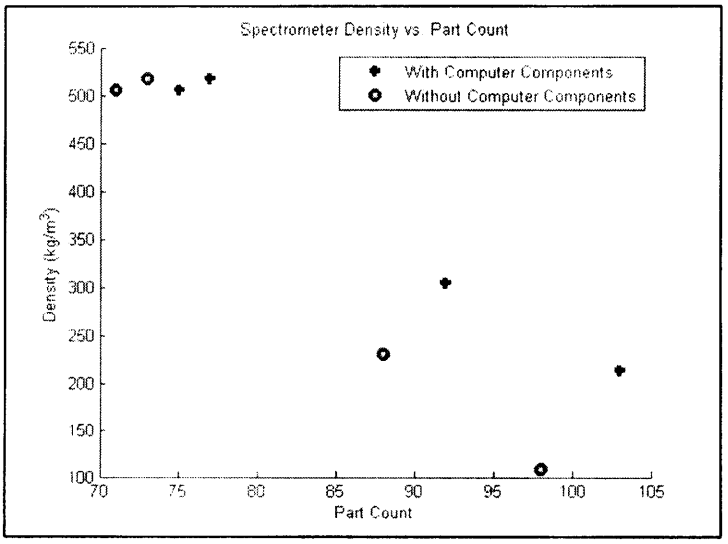

Figure 35: Spectrometer Density vs. Part Count (10)

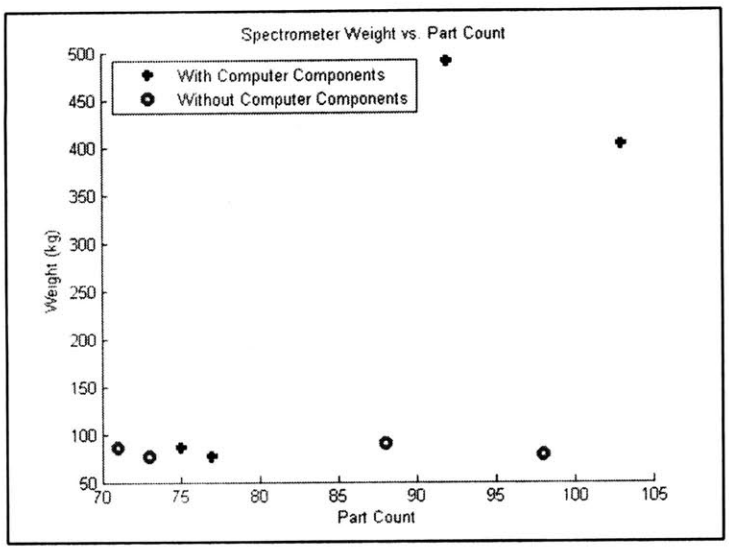

Figure 36: Spectrometer Weight vs. Part Count (10)

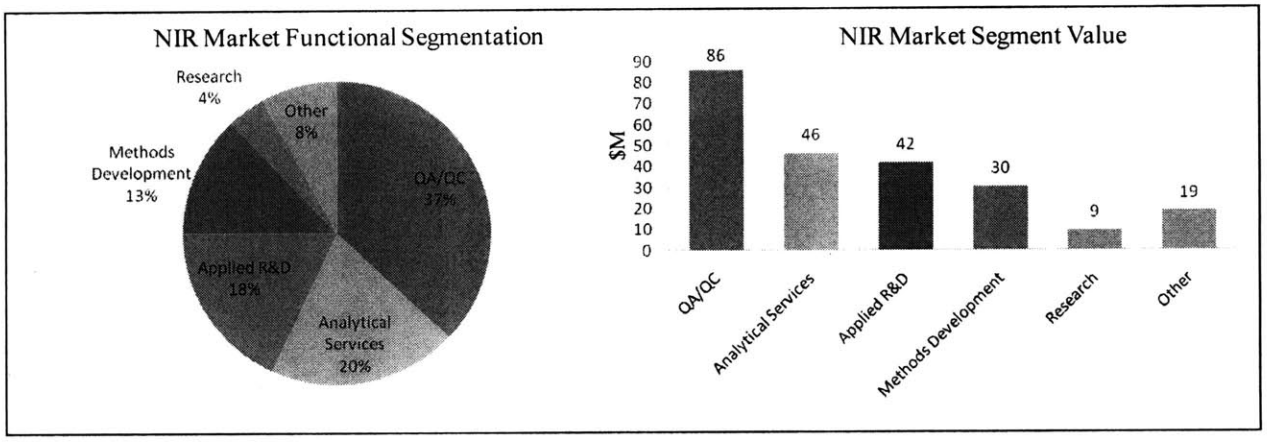

Figure 37: NIR Market Functional Segmentation (13)

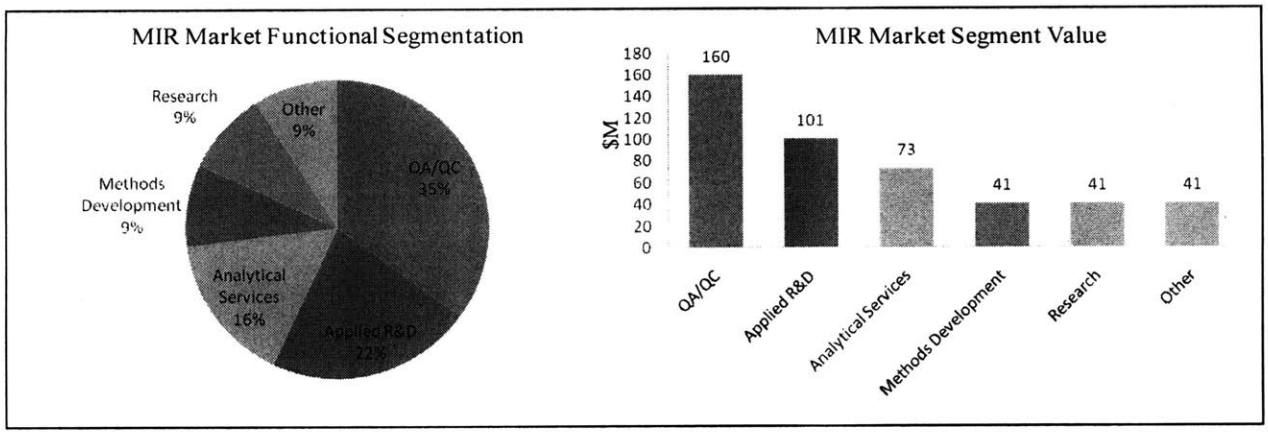

Figure 38: MIR Market Functional Segmentation (13)

7.2 Excel Data

7.2.1 Performance Data

Spectrometer Model	A	B	C	D
Year to Market	1976	1985	1988	2008
Total Spectral Range (cm)	9990.00	49990.00	49990.00	49990.00
Maximum Spectral Resolution (cm^-1)	0.04	0.12	0.10	0.07
Wavenumber Accuracy (cm^-1)	0.01	0.01	0.01	0.01
Typical SNR	500.00	6500.00	10000.00	10000.00
ADC Resolution (Bit)	12.00	16.00	16.00	24.00
Volume (m^3)	1.88	1.61	0.17	0.15
Volume Minus Computing Components (m^3)	0.72	0.39	0.17	0.15
Weight (kg)	402.00	490.00	86.00	76.36
Weight Minus Computing Components (kg)	78.00	90.00	86.00	76.36
Power Consumption (kW)	2.40	1.92	0.31	0.22
2009 Present Value Cost ($K)	2194.93	510.92	274.57	83.26
Normalized Total Spectral Range	1.0000	5.0040	5.0040	5.0040
Normalized Maximum Spectral Resolution	1.0000	2.8750	2.5000	1.7500
Normalized Wavenumber Accuracy	1.0000	1.0000	1.0000	1.0000
Normalized Typical SNR	1.0000	13.0000	20.0000	20.0000
Normalized ADC Resolution	1.0000	1.3333	1.3333	2.0000
Pspec	1.0000	30.1691	53.3760	114.3772
Pspec/Volume (m^-3)	0.5319	18.7386	313.9767	775.2771
Pspec/Volume Minus Computing (m^-3)	1.3889	77.3566	313.9767	775.2771
Pspec/Cost ($K^-1)	0.0005	0.0590	0.1944	1.3737

Table 4: Spectrometer Specifications (P_{spec} Items Highlighted) (10)

7.2.2 Design Structure Matrices

Figure 39: DSM Color-Coded Link Types

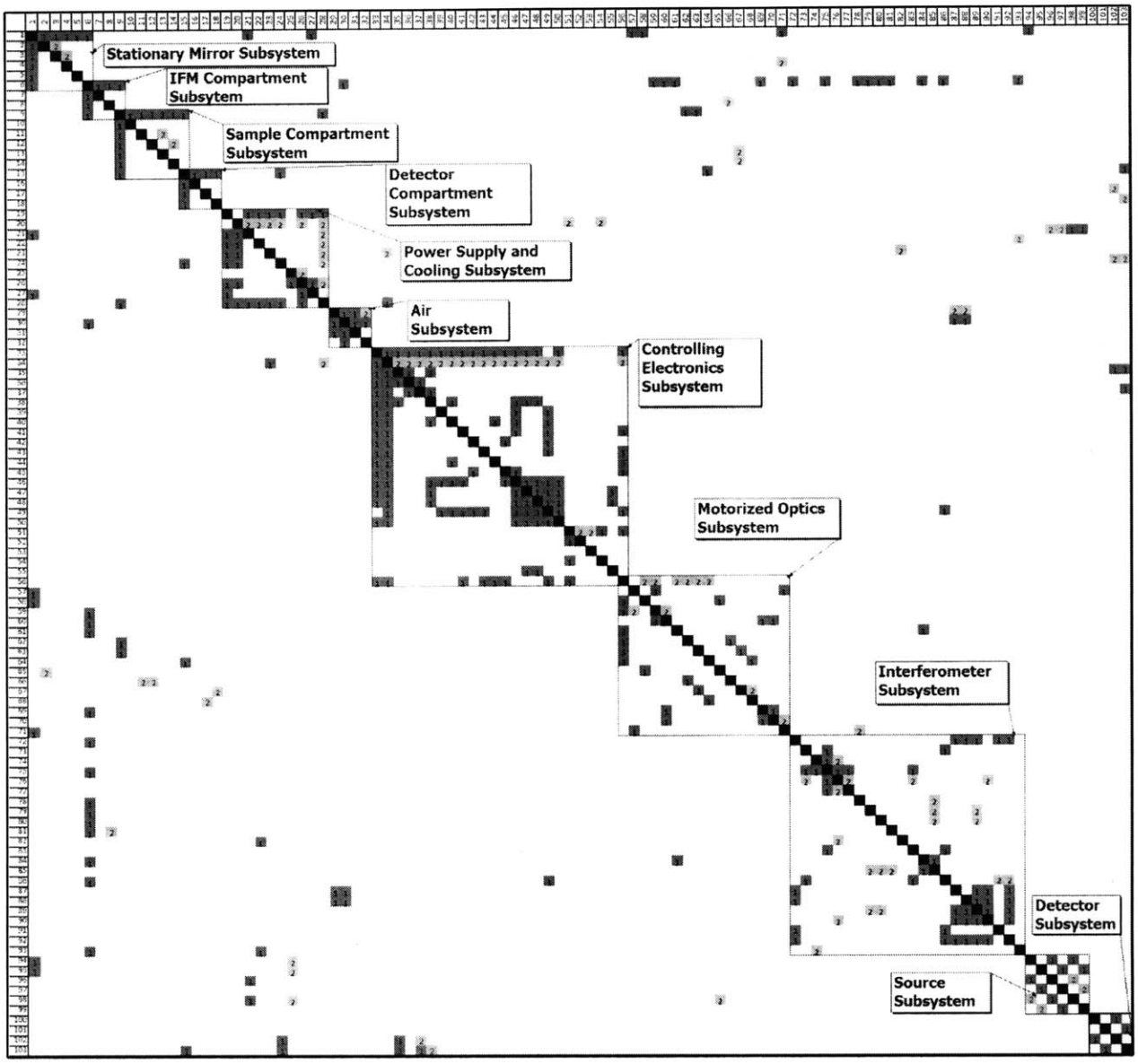

Table 5: Model A DSM (10)

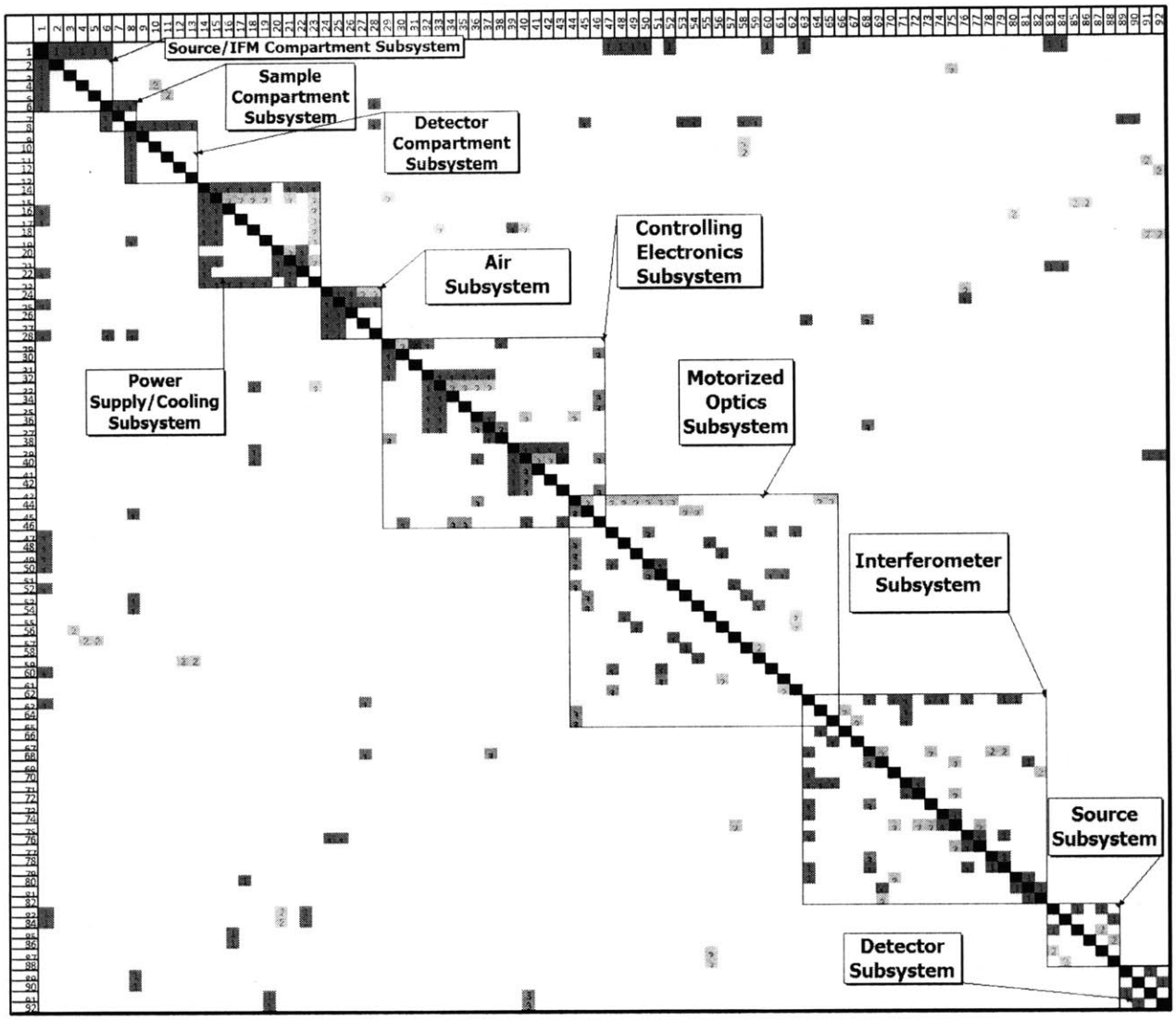

Table 6: Model B DSM (10)

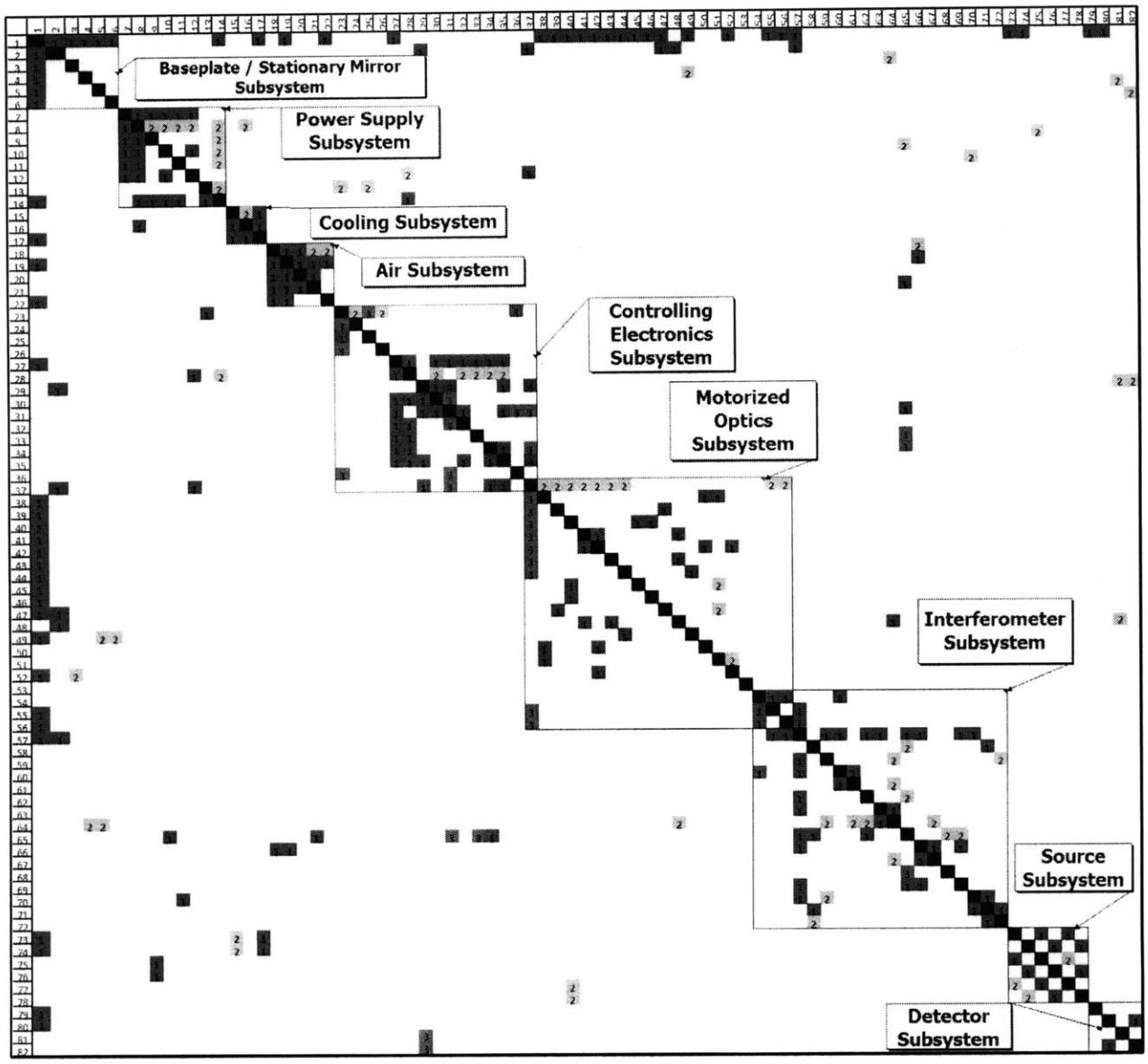

Table 7: Model C DSM (10)

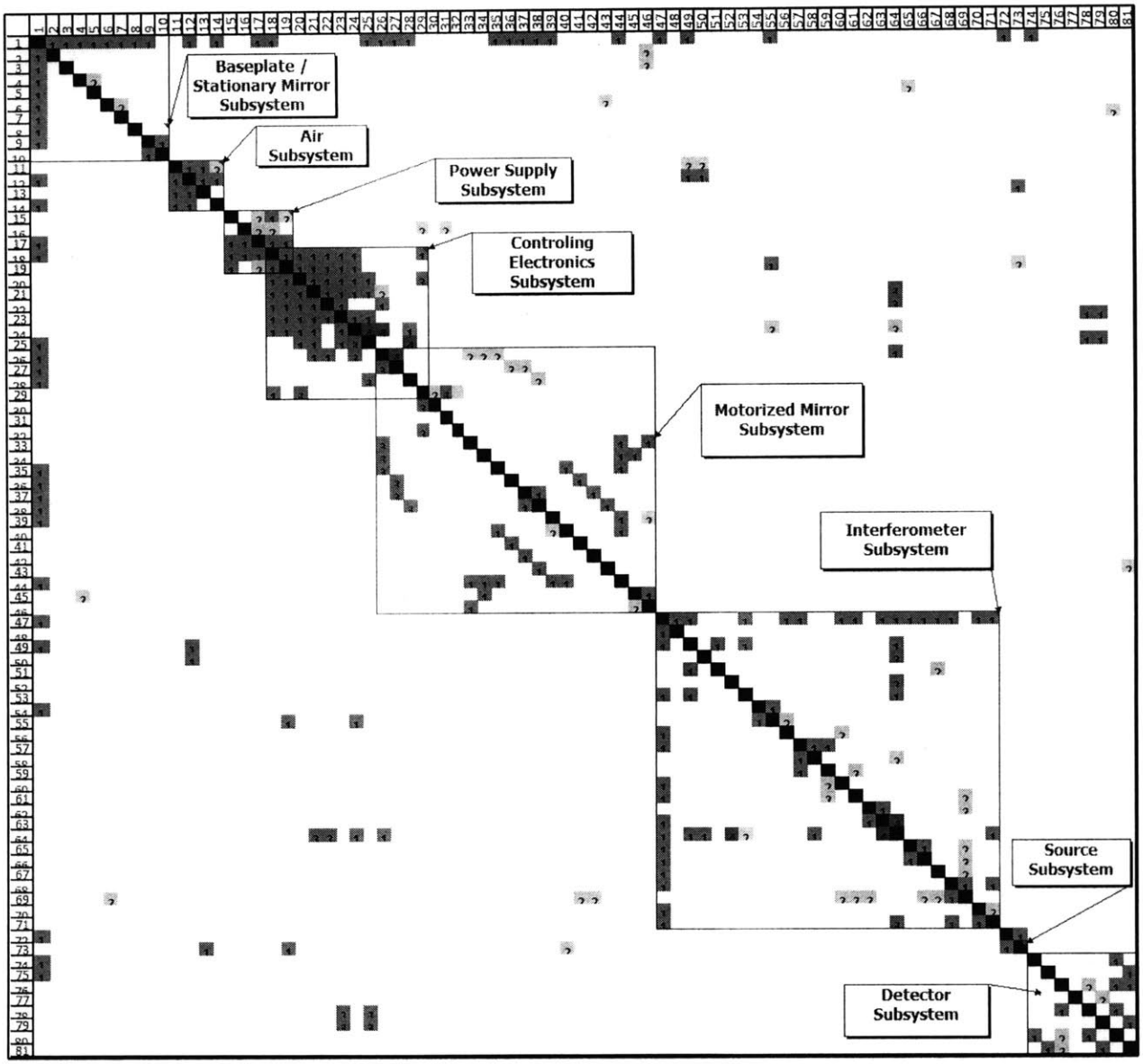

Table 8: Model D DSM (10)

7.2.3 Design Structure Matrix Analysis

Spectrometer Model	A	B	C	D
Component Count	103	92	75	77
Component Count - Computing Components	98	88	71	73
Year to Market	1976	1985	1988	2008
Total Matter Links	459	356	343	331
Total Energy Links	102	88	77	68
Total Informational Links	46	37	31	33
Total Energy & Informational Links	148	125	108	101
Matter, Energy & Information Links	0	2	3	7
Total Matter Links - Computing Links	446	344	332	320
Total Energy Links - Computing Links	98	85	73	64
Total Informational Links - Computing Links	41	34	26	28
Matter, Energy & Information Links - Computing Links	0	1	3	7

Table 9: Spectrometer DSM Data (10)

7.3 Treasury Security Interest Rates

US Treasury Security Constant Maturity Interest Rates			
Year	Rate	Year	Rate
1977	7.75	1994	7.37
1978	8.49	1995	6.88
1979	9.28	1996	6.71
1980	11.27	1997	6.61
1981	13.45	1998	5.58
1982	12.76	1999	5.87
1983	11.18	2000	5.94
1984	12.41	2001	5.49
1985	10.79	2002	5.43
1986	7.78	2003	N/D *
1987	8.59	2004	N/D *
1988	8.96	2005	N/D *
1989	8.45	2006	4.91
1990	8.61	2007	4.84
1991	8.14	2008	4.28
1992	7.67	2009	4.08
1993	6.59		
* US Treasury Constant Maturity Securites Unavailable This Year			

Table 10: Discount Rates (24)

7.4 MATLAB Code

```
function save_spec_trends(varargin)
% ------------------------------------------------------------------------
% This function reads in performance trends from an Excel file and saves
% the data in a structure to the workspace.
% ------------------------------------------------------------------------

% cd to directly of Excel file
cd('C:\Users\Tom\Desktop\Thesis\MATLAB');

% Load Excel data
specs = xlsread('performance_metrics_3_25_10.xlsx', 'Adj_Perf', 'B2:E30');
% perf_metric = xlsread('performance_metrics_3_25_10.xlsx', 'Performance
Metrics', 'H2:K13');
% adj_perf_metric = xlsread('performance_metrics_3_25_10.xlsx', 'Adj_Perf',
'B18:E18');

% Create a structure
spec_trends = struct('date','');

% Save values to structure
spec_trends.date = specs(1,:);
spec_trends.year = specs(2,:);
spec_trends.bandpass = specs(4,:);
spec_trends.res = specs(5,:);
spec_trends.w_accur = specs(6,:);
spec_trends.snr = specs(7,:);
spec_trends.adc_res = specs(9,:);
spec_trends.vol = specs(10,:);
spec_trends.vol_minus_comp = specs(11,:);
spec_trends.weight = specs(12,:);
spec_trends.weight_minus_comp = specs(13,:);
spec_trends.power = specs(14,:);
spec_trends.cost = specs(15,:);
spec_trends.pspec = specs(21,:);
spec_trends.adj_pspec = specs(22,:);
spec_trends.norm_pspec = specs(23,:);
spec_trends.pspec_over_vol = specs(24,:);
spec_trends.pspec_over_vol_minus_comp = specs(25,:);
spec_trends.pspec_over_cost = specs(26,:);
spec_trends.norm_pspec_over_vol = specs(27,:);
spec_trends.norm_pspec_over_vol_minus_comp = specs(28,:);
spec_trends.norm_pspec_over_cost = specs(29,:);

filename = ['spec_trends_',date];

% Save specs variable
save(filename, 'spec_trends');

end
```

```
function dsm_analysis(varargin)
% ------------------------------------------------------------------------
% This function reads in the DSM excel files for the four systems, extracts
% architecture trends, writes them to an excel file, and saves them as a
% structure to the workspace.
% ------------------------------------------------------------------------
cd('C:\Users\Tom\Desktop\Thesis\DSM\Merged DSMs');
% Load excel table
model_a = xlsread('model_a_merged_DSM_2_19_10.xlsx','Merged','B2:CZ104');
model_b = xlsread('model_b_merged_DSM_2_19_10.xlsx','Merged','B2:CO93');
model_c = xlsread('model_c_merged_DSM_2_19_10.xlsx','Merged','B2:CE83');
model_d = xlsread('model_d_merged_DSM_2_19_10.xlsx','Merged','B2:CD82');


% Eliminate NaNs
[m_a n_a] = find(~isnan(model_a));
[m_b n_b] = find(~isnan(model_b));
[m_c n_c] = find(~isnan(model_c));
[m80 n_d] = find(~isnan(model_d));

dsm__a = zeros(length(model_a));
dsm__b = zeros(length(model_b));
dsm__c = zeros(length(model_c));
dsm__d = zeros(length(model_d));

for ii = 1:length(m_a)
    dsm__a(m_a(ii),n_a(ii)) = model_a(m_a(ii),n_a(ii));
end

for ll = 1:length(m_b)
    dsm__b(m_b(ll),n_b(ll)) = model_b(m_b(ll),n_b(ll));
end

for jj = 1:length(m_c)
    dsm__c(m_c(jj),n_c(jj)) = model_c(m_c(jj),n_c(jj));
end

for kk = 1:length(m_d)
    dsm__d(m_d(kk),n_d(kk)) = model_d(m_d(kk),n_d(kk));
end

% Find total matter, energy, and informational links.
jmind__a = find(dsm__a == 1);
mind__a = find(dsm__a == 1 | dsm__a == 2 | dsm__a == 3 | dsm__a == 4);
eind__a = find(dsm__a == 2 | dsm__a == 4);
iind__a = find(dsm__a == 3 | dsm__a == 4);

jmind__b = find(dsm__b == 1);
mind__b = find(dsm__b == 1 | dsm__b == 2 | dsm__b == 3 | dsm__b == 4);
eind__b = find(dsm__b == 2 | dsm__b == 4);
iind__b = find(dsm__b == 3 | dsm__b == 4);
```

```
jmind_c = find(dsm_c == 1);
mind_c = find(dsm_c == 1 | dsm_c == 2 | dsm_c == 3 | dsm_c == 4);
eind_c = find(dsm_c == 2 | dsm_c == 4);
iind_c = find(dsm_c == 3 | dsm_c == 4);

jmind_d = find(dsm_d == 1);
mind_d = find(dsm_d == 1 | dsm_d == 2 | dsm_d == 3 | dsm_d == 4);
eind_d = find(dsm_d == 2 | dsm_d == 4);
iind_d = find(dsm_d == 3 | dsm_d == 4);

% Find just combination of links
meind_a = find(dsm_a == 2);
miind_a = find(dsm_a == 3);
meiind_a = find(dsm_a == 4);

meind_b = find(dsm_b == 2);
miind_b = find(dsm_b == 3);
meiind_b = find(dsm_b == 4);

meind_c = find(dsm_c == 2);
miind_c = find(dsm_c == 3);
meiind_c = find(dsm_c == 4);

meind_d = find(dsm_d == 2);
miind_d = find(dsm_d == 3);
meiind_d = find(dsm_d == 4);

% Find the densities
mden_a = length(mind_a)/(length(model_a)^2-length(model_a));
eden_a = length(eind_a)/(length(model_a)^2-length(model_a));
iden_a = length(iind_a)/(length(model_a)^2-length(model_a));
cden_a = length(meiind_a)/(length(model_a)^2-length(model_a));

mden_b = length(mind_b)/(length(model_b)^2-length(model_b));
eden_b = length(eind_b)/(length(model_b)^2-length(model_b));
iden_b = length(iind_b)/(length(model_b)^2-length(model_b));
cden_b = length(meiind_b)/(length(model_b)^2-length(model_b));

mden_c = length(mind_c)/(length(model_c)^2-length(model_c));
eden_c = length(eind_c)/(length(model_c)^2-length(model_c));
iden_c = length(iind_c)/(length(model_c)^2-length(model_c));
cden_c = length(meiind_c)/(length(model_c)^2-length(model_c));

mden_d = length(mind_d)/(length(model_d)^2-length(model_d));
eden_d = length(eind_d)/(length(model_d)^2-length(model_d));
iden_d = length(iind_d)/(length(model_d)^2-length(model_d));
cden_d = length(meiind_d)/(length(model_d)^2-length(model_d));

% Combine all data
data_a = [length(mind_a); length(eind_a);
    length(iind_a); length(jmind_a); length(meind_a);
    length(miind_a); length(meiind_a); mden_a; eden_a;
    iden_a; cden_a];
data_b = [length(mind_b); length(eind_b);
    length(iind_b); length(jmind_b); length(meind_b);
```

```
    length(miind_b); length(meiind_b); mden_b; eden_b;
    iden_b; cden_b];
data_c = [length(mind_c); length(eind_c);
    length(iind_c); length(jmind_c); length(meind_c);
    length(miind_c); length(meiind_c); mden_c; eden_c;
    iden_c; cden_c];
data_d = [length(mind_d); length(eind_d);
    length(iind_d); length(jmind_d); length(meind_d);
    length(miind_d); length(meiind_d); mden_d; eden_d;
    iden_d; cden_d];

% Enter values to be plotted
% First browse to excel file path
cd('C:\Users\Tom\Desktop\Thesis\MATLAB\');

% Write to excel
xlswrite('dsm_analysis_2_19_10.xlsx',data_a,'Plots','b20:b30');
xlswrite('dsm_analysis_2_19_10.xlsx',data_b,'Plots','c20:c30');
xlswrite('dsm_analysis_2_19_10.xlsx',data_c,'Plots','d20:d30');
xlswrite('dsm_analysis_2_19_10.xlsx',data_d,'Plots','e20:e30');

% Save the data to structures
filename = ['dsm_data_', date];
dsm_data = struct('model_a', data_a, 'model_b', data_b, 'model_c', data_c,
'model_d', data_d);
save (filename, 'dsm_data');

end
```

```
function save_dsm_trends(varargin)
% ------------------------------------------------------------------------
% This function reads in performance trends from an Excel file and saves
% them to an structure in the workspace.
% ------------------------------------------------------------------------

% cd to directly of Excel file
cd('C:\Users\Tom\Desktop\Thesis\MATLAB');

% Load Excel data
links = xlsread('dsm_analysis_3_25_10.xlsx', 'Plots', 'B2:E44');

% Create a structure
dsm_trends = struct('date','');

% Save values to structure
dsm_trends.date = [1974 1985 1988 2008];
dsm_trends.year = [0 9 12 32];
dsm_trends.part_count = links(1,:);
dsm_trends.mod_count = links(3,:);
dsm_trends.tot_mat = links(19,:);
dsm_trends.tot_energy = links(20,:);
dsm_trends.tot_info = links(21,:);
```

```
dsm_trends.mat = links(22,:);
dsm_trends.mat_en = links(23,:);
dsm_trends.mat_info = links(24,:);
dsm_trends.mat_en_info = links(25,:);
dsm_trends.mat_dens = links(26,:);
dsm_trends.en_dens = links(27,:);
dsm_trends.info_dens = links(28,:);
dsm_trends.comb = links(29,:);

dsm_trends.part_count_minus_comp = links(2,:);
dsm_trends.tot_mat_minus_comp = links(30,:);
dsm_trends.tot_energy_minus_comp = links(31,:);
dsm_trends.tot_info_minus_comp = links(32,:);
dsm_trends.mat_minus_comp = links(33,:);
dsm_trends.mat_en_minus_comp = links(34,:);
dsm_trends.mat_info_minus_comp = links(35,:);
dsm_trends.mat_en_info_minus_comp = links(36,:);

dsm_trends.rel_en_dens = links(37,:);
dsm_trends.rel_info_dens = links(38,:);
dsm_trends.rel_en_info_dens = links(39,:);
dsm_trends.mat_prop = links(41,:);
dsm_trends.en_prop = links(42,:);
dsm_trends.info_prop = links(43,:);

filename = ['dsm_trends_',date];

% Save dsm_trends variable
save(filename, 'dsm_trends');

end


function plot_dsm_trends(varargin)
% -------------------------------------------------------------------------
% This function loads dsm_trends structure from the workspace and plots the
% data.
% -------------------------------------------------------------------------

% Load data
cd('C:\Users\Tom\Desktop\Thesis\MATLAB');
load('dsm_trends_01-Apr-2010.mat');

time = dsm_trends.year;

% Part Count vs Time
figure;
hold on;
plot(time, dsm_trends.part_count, 'k+','Markersize', 6, 'LineWidth', 3);
plot(time, dsm_trends.part_count_minus_comp, 'ro','Markersize', 6,
'LineWidth', 3);
title('Spectrometer Component Count vs. Time');
legend('With Computer Components','Without Computer Components');
xlabel('Years After 1976 (Yr)');
ylabel('Component Count');
```

```
xlim([-5,40]);
ylim([65,110]);

% Matter/Spatial Links vs Time
figure;
hold on;
plot(time, dsm_trends.tot_mat, 'k+','Markersize', 6, 'LineWidth', 3);
plot(time, dsm_trends.tot_mat_minus_comp, 'ro','Markersize', 6, 'LineWidth',
3);
title('Spectrometer Matter/Spatial Links vs. Time');
legend('With Computer Components','Without Computer Components');
xlabel('Years After 1976 (Yr)');
ylabel('Matter/Spatial Links');
xlim([-5,40]);
ylim([300,480]);

% Energy Links vs Time
figure;
hold on;
plot(time, dsm_trends.tot_energy, 'k+','Markersize', 6, 'LineWidth', 3);
plot(time, dsm_trends.tot_energy_minus_comp, 'ro','Markersize', 6,
'LineWidth', 3);
title('Spectrometer Energy Links vs. Time');
legend('With Computer Components','Without Computer Components');
xlabel('Years After 1976 (Yr)');
ylabel('Energy Links');
xlim([-5,40]);

% Info Links vs Time
figure;
hold on;
plot(time, dsm_trends.tot_info, 'k+','Markersize', 6, 'LineWidth', 3);
plot(time, dsm_trends.tot_info_minus_comp, 'ro','Markersize', 6, 'LineWidth',
3);
title('Spectrometer Info Links vs. Time');
legend('With Computer Components','Without Computer Components');
xlabel('Years After 1976 (Yr)');
ylabel('Info Links');
xlim([-5,40]);
ylim([23,50]);

% Energy/Info Links vs Time
figure;
hold on;
plot(time, dsm_trends.tot_info+dsm_trends.tot_energy, 'k+','Markersize', 6,
'LineWidth', 3);
plot(time, dsm_trends.tot_info_minus_comp+dsm_trends.tot_energy_minus_comp,
'ro','Markersize', 6, 'LineWidth', 3);
title('Spectrometer Energy/Info Links vs. Time');
legend('With Computer Components','Without Computer Components');
xlabel('Years After 1976 (Yr)');
ylabel('Info/Energy Links');
xlim([-5,40]);

end
```

```
function plot_spec_trends(varargin)
% ------------------------------------------------------------------------
% This function loads spec_trends from the workspace and plots the data.
% ------------------------------------------------------------------------

cd('C:\Users\Tom\Desktop\Thesis\MATLAB');

load('spec_trends_01-Apr-2010.mat');

time = spec_trends.year;

% Normalized Pspec vs Time
figure;
hold on;
plot(time, spec_trends.norm_pspec, 'k+','Markersize', 6, 'LineWidth', 3);
title('Pspec vs. Time');
legend('Pspec');
xlabel('Years After 1976 (yr)');
ylabel('Pspec Value');
xlim([-5,40]);
ylim([-10,125]);

% Ln(Normalized Pspec) vs Time
figure;
hold on;
plot(time, log(spec_trends.norm_pspec), 'k+','Markersize', 6, 'LineWidth',
3);
title('Ln(Pspec) vs. Time');
% legend('Ln(Pspec)');
xlabel('Years After 1976 (yr)');
ylabel('Ln(Pspec Value)');
xlim([-5,40]);
ylim([-0.5,5.5]);

% Normalize Pspec over Volume vs Time
figure;
hold on;
plot(time, spec_trends.norm_pspec_over_vol, 'k+','Markersize', 6,
'LineWidth', 3);
plot(time, spec_trends.norm_pspec_over_vol_minus_comp, 'ro','Markersize', 6,
'LineWidth', 3);
title('Pspec/Volume vs. Time');
legend('With Computing Components','Without Computing Components');
xlabel('Years After 1976 (yr)');
ylabel('Pspec Per m^3');
xlim([-5,40]);
ylim([-60,850]);

% Ln(Normalize Pspec over Volume) vs Time
figure;
hold on;
plot(time, log(spec_trends.norm_pspec_over_vol), 'k+','Markersize', 6,
'LineWidth', 3);
```

```
plot(time, log(spec_trends.norm_pspec_over_vol_minus_comp),
'ro','Markersize', 6, 'LineWidth', 3);
title('Ln(Pspec/Volume) vs. Time');
legend('With Computing Components','Without Computing Components');
xlabel('Years After 1976 (yr)');
ylabel('Ln(Pspec Per m^3)');
xlim([-5,40]);
ylim([-1.5,7.5]);

% Normalize Pspec over Cost vs Time
figure;
hold on;
plot(time, spec_trends.norm_pspec_over_cost, 'k+','Markersize', 6,
'LineWidth', 3);
title('Pspec/Cost vs. Time');
legend('With Computing Components');
xlabel('Years After 1976 (yr)');
ylabel('Pspec Per $K');
xlim([-5,40]);
ylim([-0.15,1.6]);

% Ln(Normalize Pspec over Cost) vs Time
figure;
hold on;
plot(time, log(spec_trends.norm_pspec_over_cost), 'k+','Markersize', 6,
'LineWidth', 3);
title('Ln(Pspec/Cost) vs. Time');
legend('With Computing Components');
xlabel('Years After 1976 (yr)');
ylabel('Ln(Pspec Per $K)');
xlim([-5,40]);
ylim([-8.5,1]);

% Volume vs Time
figure;
hold on;
plot(time, spec_trends.vol, 'k+','Markersize', 6, 'LineWidth', 3);
plot(time, spec_trends.vol_minus_comp, 'ro','Markersize', 6, 'LineWidth', 3);
title('Spectrometer Volume vs. Time');
legend('With Computer Components','Without Computer Components');
xlabel('Years After 1976 (Yr)');
ylabel('Volume (m^3)');
xlim([-5,40]);

% Weight vs Time
figure;
hold on;
plot(time, spec_trends.weight, 'k+','Markersize', 6, 'LineWidth', 3);
plot(time, spec_trends.weight_minus_comp, 'ro','Markersize', 6, 'LineWidth',
3);
title('Spectrometer Weight vs. Time');
legend('With Computer Components','Without Computer Components');
xlabel('Years After 1976 (Yr)');
ylabel('Weight (kg)');
xlim([-5,40]);
```

```
% Density vs Time
figure;
hold on;
plot(time, (spec_trends.weight)./spec_trends.vol, 'k+','Markersize', 6,
'LineWidth', 3);
plot(time, (spec_trends.weight_minus_comp)./spec_trends.vol_minus_comp,
'ro','Markersize', 6, 'LineWidth', 3);
title('Spectrometer Density vs. Time');
legend('With Computer Components','Without Computer Components');
xlabel('Years After 1976 (Yr)');
ylabel('Density (kg/m^3)');
xlim([-5,40]);
ylim([50,560]);

% Power Consumption vs Time
figure;
hold on;
plot(time, spec_trends.power, 'k+','Markersize', 6, 'LineWidth', 3);
% plot(time, spec_trends.power_minus_comp, 'ro','Markersize', 6, 'LineWidth',
3);
title('Spectrometer Power Consumption vs. Time');
legend('With Computer Components');
xlabel('Years After 1976 (Yr)');
ylabel('Power Consumption (kW)');
xlim([-5,40]);
ylim([0,2.7]);

% Cost vs Time
figure;
hold on;
plot(time, spec_trends.cost, 'k+','Markersize', 6, 'LineWidth', 3);
% plot(time, spec_trends.cost, 'ro','Markersize', 6, 'LineWidth', 3);
title('Spectrometer Cost vs. Time');
legend('With Computer Components');
xlabel('Years After 1976 (Yr)');
ylabel('Present Value Cost ($K)');
xlim([-5,40]);

% Ln(Cost) vs Time
figure;
hold on;
plot(time, log(spec_trends.cost), 'k+','Markersize', 6, 'LineWidth', 3);
% plot(time, spec_trends.cost, 'ro','Markersize', 6, 'LineWidth', 3);
title('Ln(Spectrometer Cost) vs. Time');
legend('With Computer Components');
xlabel('Years After 1976 (Yr)');
ylabel('Ln(Present Value Cost ($K))');
xlim([-5,40]);

end
```

```
function plot_correlations(varargin)
% ------------------------------------------------------------------------
% This function loads both spec_trends and dsm_trends from the workspace
% and plots correlation data.
% ------------------------------------------------------------------------

cd('C:\Users\Tom\Desktop\Thesis\MATLAB');

load('spec_trends_01-Apr-2010.mat');
load('dsm_trends_01-Apr-2010.mat');

time = spec_trends.year;

% Cost vs. Matter Links
figure;
hold on;
plot(dsm_trends.tot_mat, spec_trends.cost,'k+','Markersize', 6, 'LineWidth',
3);
title('Spectrometer Cost vs. Matter/Spatial Links');
xlabel('Matter/Spatial Links');
ylabel('2009 Present Value Cost ($K)');
xlim([310,480]);
ylim([-200,2500]);

% Volume vs. Part Count
figure;
hold on;
plot(dsm_trends.part_count, spec_trends.vol, 'k+','Markersize', 6,
'LineWidth', 3);
plot(dsm_trends.part_count_minus_comp, spec_trends.vol_minus_comp,
'ro','Markersize', 6, 'LineWidth', 3);
title('Spectrometer Volume vs. Component Count');
legend('With Computer Components','Without Computer Components');
xlabel('Part Count');
ylabel('Volume (m^3)');
xlim([65,110]);
ylim([-0.1,2.2]);

% Weight vs. Part Count
figure;
hold on;
plot(dsm_trends.part_count, spec_trends.weight, 'k+','Markersize', 6,
'LineWidth', 3);
plot(dsm_trends.part_count_minus_comp, spec_trends.weight_minus_comp,
'ro','Markersize', 6, 'LineWidth', 3);
title('Spectrometer Weight vs. Part Count');
legend('With Computer Components','Without Computer Components');
xlabel('Part Count');
ylabel('Weight (kg)');

% Density vs. Part Count
figure;
```

```
hold on;
plot(dsm_trends.part_count, (spec_trends.weight)./spec_trends.vol,
'k+','Markersize', 6, 'LineWidth', 3);
plot(dsm_trends.part_count_minus_comp,
(spec_trends.weight_minus_comp)./spec_trends.vol_minus_comp,
'ro','Markersize', 6, 'LineWidth', 3);
title('Spectrometer Density vs. Part Count');
legend('With Computer Components','Without Computer Components');
xlabel('Part Count');
ylabel('Density (kg/m^3)');

% Power vs. Info Links
figure;
hold on;
plot(dsm_trends.tot_info, spec_trends.power, 'k+','Markersize', 6,
'LineWidth', 3);
% plot(dsm_trends.tot_info_minus_comp, spec_trends.power, 'ro','Markersize',
6, 'LineWidth', 3);
title('Spectrometer Power Consumption vs. Info Links');
legend('With Computer Components');
xlabel('Info Links');
ylabel('Power Consumption (kW)');

% Power vs. Energy Links
figure;
hold on;
plot(dsm_trends.tot_energy, spec_trends.power, 'k+','Markersize', 6,
'LineWidth', 3);
% plot(dsm_trends.tot_energy_minus_comp, spec_trends.power,
'ro','Markersize', 6, 'LineWidth', 3);
title('Spectrometer Power Consumption vs. Energy Links');
legend('With Computer Components');
xlabel('Energy Links');
ylabel('Power Consumption (kW)');

% Power vs. Energy/Info Links
figure;
hold on;
plot((dsm_trends.tot_energy+dsm_trends.tot_info), spec_trends.power,
'k+','Markersize', 6, 'LineWidth', 3);
% plot(dsm_trends.part_count_minus_comp,
(spec_trends.weight_minus_comp)./spec_trends.vol_minus_comp, 'ro-
','Markersize', 6, 'LineWidth', 3);
title('Spectrometer Power Consumption vs. Energy/Info Links');
legend('With Computer Components');
xlabel('Energy and Information Links');
ylabel('Power Consumption (kW)');
xlim([90,155]);
ylim([-0.2,2.7]);

% Power vs. Part Count
figure;
hold on;
plot((dsm_trends.part_count), spec_trends.power, 'k+','Markersize', 6,
'LineWidth', 3);
```

```
% plot(dsm_trends.part_count_minus_comp, (spec_trends.power),
'ro','Markersize', 6, 'LineWidth', 3);
title('Spectrometer Power Consumption vs. Part Count');
legend('With Computer Components');
xlabel('Part Count');
ylabel('Power Consumption (kW)');

end
```

8 Bibliography

1. **Sheffield Hallam University Biosciences.** Infra-Red Absorption Spectroscopy - Theoretical Principles. *Sheffield Hallam University Biosciences Online Learning.* [Online] 2010. [Cited: January 28, 2010.] http://teaching.shu.ac.uk/hwb/chemistry/tutorials/molspec/irspec1.htm.

2. **Reusch, William, PhD.** Infrared Spectroscopy. *Michigan State University's Virtual Text of Organic Chemistry.* [Online] August 10, 2007. [Cited: January 28, 2010.] http://www.cem.msu.edu/~reusch/VirtualText/Spectrpy/InfraRed/infrared.htm#.

3. *Rapid Scan Infrared Spectrometer for Operation with Support Coated Open Tubular or Packed Column Gas Chromatographs.* **Brown et al, R. A.** 1971, Analytical Chemistry, p. 354.

4. **Polychromix.** Polychromix MEMS NIR - How does this technology work? What are the advatages? *www.polychromix.com.* [Online] July 27, 2009. [Cited: April 14, 2010.] http://www.polychromix.com/PDF/AN99-MEMSTechnology%20Overview.pdf.

5. **Thermo Nicolet Corp.** *Introduction to Fourier Transform Infrared Spectrometry.* Madison, WI : Thermo Nicolet Corporation, 2001.

6. **Encylopedia Brittannica.** Michelson-Morley Experiment. *Encylopedia Britannica Online.* [Online] 2010. [Cited: February 8, 2010.] http://www.britannica.com/EBchecked/topic/380069/Michelson-Morley-experiment#ref=ref286117.

7. **Newport Corporation.** Introduction to FTIR Spectroscopy. *www.newport.com.* [Online] 2010. [Cited: March 10, 2010.] http://www.newport.com/Introduction-to-FT-IR-Spectroscopy/405840/1033/catalog.aspx#.

8. **Griffiths and Haseth.** *Fourier Transform Infrared Spectroscopy.* Hoboken, NJ : Wiley, 2007.

9. **Smith, Brian.** *Fundamentals of Fourier Transform Infrared Spectroscopy.* Boca Raton, FL : CRC Press, 1996.

10. **Bruker Optics Inc.**

11. **Mattox, Donald.** Historical Timeline of Vacuum Coating and Vacuum/Plasma Technology. *Society of Vacuum Coaters.* [Online] 2003. [Cited: February 8, 2010.] http://www.svc.org/HistoryofVacuumCoating/History-of-Vacuum-Coating.cfm.

12. **Schmid, Lawrence.** Spectroscopy: Enduring During Uncertain Times. *Spectroscopy.* March 1, 2009.

13. **SDI Inc.** *Global Assessment Report 10.5.* Los Angeles, CA : Strategic Directions International Inc, 2009.

14. **Shimadzu Corporation.** FTIR Talk Letter Vol. 4. *shimadzu.co.* [Online] May 2006. [Cited: February 27, 2010.] http://www2.shimadzu.com/applications/FTIR/FTIR_TalkLetter_Vol_4.pdf.

15. **Lindemann.** Design Structure Matrix. *www.dsmweb.org.* [Online] 2009. [Cited: April 14, 2010.] http://129.187.108.94/dsmweb/en/dsm.html.

16. —. Different DSM Types. *www.dsmweb.org.* [Online] 2009. [Cited: April 14, 2010.] http://129.187.108.94/dsmweb/en/understand-dsm/technical-dsm-tutorial0/different-dsm-types.html.

17. *Complex System Classification.* **Magee and Weck, de.** 2004. INCOSE. p. 14.

18. *Integration Analysis of Product Decompositions.* **Pimmler and Eppinger.** Minneapolis, MN : s.n., 1994. ASME Design Theory and Methodology Conference. p. 4.

19. **Kaplan.** Innovation Lifecycles. *www.innovation-point.com.* [Online] 2007. [Cited: April 14, 2010.] http://www.innovation-point.com/Innovation_Lifecycles.pdf.

20. **Holwerda.** Father of the Altair 8800, Ed Roberts, Passes Away. *www.osnews.com.* [Online] April 2, 2010. [Cited: April 14, 2010.] http://www.osnews.com/story/23100/Father_of_the_Altair_8800_Ed_Roberts_Passes_Away.

21. **Epner Technology.** Laser Gold Properites. [Online] 2004. [Cited: March 29, 2010.] http://www.epner.com/laser_properties.ssi#.

22. **Analog Devices.** *Data Converter History.* s.l. : Analog Devices, 2004.

23. **SDI Inc.** *Worldwide Molecular Spectrscopy Survey - Corroborating Market Trends and Revealing End-Use Opinions.* Los Angeles, CA : SDI Inc., 2008.

24. **US Federal Reserve.** Market Yield on US Treasury Securities at 30-Year Constant Maturity. *www.federalreserve.gov.* [Online] http://www.federalreserve.gov/releases/h15/data/Annual/H15_TCMNOM_Y30.txt.

25. **Varian Inc.** The History of Varian FT-IR Spectrometers. *www.varianinc.com.* [Online] 2008. [Cited: February 8, 2010.] http://www.varianinc.com/image/vimage/docs/applications/apps/si-0260.pdf.

26. **PerkinElmer.** 60 Years of PerkinElmer Innovation in Infrared Spectroscopy. *www.perkinelmer.com.* [Online] 2005. [Cited: February 8, 2010.] http://las.perkinelmer.com/content/relatedmaterials/brochures/bro_60yearsinfraredspectroscopy.pdf.

27. **Da Cruz, Frank.** Columbia University Computing History. *The IBM 610 Auto-Point Computer.* [Online] April 29, 2009. [Cited: February 8, 2010.] http://www.columbia.edu/acis/history/610.html.

28. **Polychromix.** PHAZIR Handheld NIR Material Analyzer. *www.polychromix.com.* [Online] 11 7, 2007. [Cited: April 13, 2010.] http://www.polychromix.com/PDF/phazir.pdf.

29. **Axsun Technologies.** Spectroscopy Products. *www.axsun.com.* [Online] March 5, 2007. [Cited: April 13, 2010.] http://www.axsun.com/html/products_spectroscopy.htm.

30. **Salzer, Reiner and Siesler, Heinz.** *Infrared and Raman Spectroscopic Imaging.* Weinheim : Wiley - VCH, 2009. p. 45.

31. *Gauss and the History of the Fast Fourier Transform.* **Heideman, Johnson and Burrus.** 1985, Archive for History of Exact Sciences, pp. 1, 266.

32. **Chapman, Allan.** William Lassell (1799-1880) and the Discovery of Triton, 1846. [Online] October 4, 2005. [Cited: April 14, 2010.] http://www.mikeoates.org/lassell/lassell_by_a_chapman.htm.

33. **Photonics.** Phazir handheld NIR Spectrometer. *www.photonics.com.* [Online] May 17, 2006. [Cited: April 14, 2010.] http://www.photonics.com/Article.aspx?AID=25502.